Machining of titanium alloys using WC cutting tools – conventional vs. 3D printed Ti-6Al-4V

Jordan Colussi

Bachelor of Engineering
Mechanical Engineering

MACQUARIE
University
SYDNEY·AUSTRALIA

Department of Engineering
Macquarie University

October 11th, 2016

Supervisor: Dr. Wei Xu

1

Acknowledgements

I would like to acknowledge several staff of the Department of Engineering; Dr. Wei Xu, Prof. Candace Lang, and Dr. Nicholas Tse. After the initial project supervisor left the department, these members of staff have encouraged and made the effort to ensure this unfortunate event does not hinder my ability to complete the thesis research topic to the best of my ability.

The staff from the microscopy labs – Sue Lindsay and Nadia Suarez-Bosche for helping me with all analysis that I required.

Statement of Candidate

I, Jordan Colussi, declare that this report, submitted as part of the requirement for the award of Bachelor of Engineering in the Department of Mechanical Engineering, Macquarie University, is entirely my own work unless otherwise referenced or acknowledged. This document has not been submitted for qualification or assessment at any academic institution.

Student's Name: Jordan Colussi

Student's Signature: Jordan Colussi (electronic)

Date: October 11, 2016

Abstract

The advancement of material science led to the introduction of 3D printing metals. One of these metals, Titanium, is a material with the best weight to strength ratio of any metal. As it is expensive to manufacture, 3D printing aims to create intricate components that would normally be uneconomically viable.

3D printing does not yet produce parts with a good quality surface finish, hence requiring machining to get the desired finish. With little information on how to machine the 3D printed material, the thesis sets out to investigate whether the machining parameters typically used for commercial grade are suitable for 3D printed titanium.

The project involves lathe machining both commercial grade and SLM 3D Printed Ti-6Al-4V and using different cutting tools at different machining parameters to find trends and the most optimal cutting procedure. Electron microscopes (SEM) and compositional analysis (EDS) is used to analyse the specimens to confirm if any diffusion or premature wearing of the carbide occurred.

As 3D Printed Titanium is a much harder material than commercial grade, the coating failed and large built up edges formed on the cutting tools. No diffusion was found on the uncoated cutting tools; the coating on the cutting tool, titanium, is the same as the machined metal, it is inconclusive if diffusion occurred.

3D printing requires decades of innovation before it is at a standard where processing no longer required. Until then machining will remain as post processing method. Effective machining will introduce the widespread use of 3D printed specimens and minimize the downsides of such manufacturing methods.

Contents

List of Figures

List of Tables

1. Introduction

The world relies on metals to build infrastructure, vehicles, electronic devices and implants; as technology increases, the demand for stronger and lighter-weight materials becomes prevalent. When these materials are invented/discovered, it needs to be cost effective to implement in commonplace. Implementing new materials relies on economic viability of producing the raw material, and then being able to process the raw material into the finished final product.

Titanium, most commonly produced as an alloy, is found in state-of-the-art projects developed by the aerospace, high end automotive, biomedical and petroleum industries [1] [2]; where cost is not paramount. This high cost comes from the processing of the raw material [3]. New procedures like selective laser melting (SLM), a 3D printing process, aim to reduce the cost of manufacturing, but result in imperfect microstructures and a poor surface finish, which then similarly requires further processing such as machining [4].

Machining will always remain within the manufacturing industry, as it is so versatile. However, the machining process of titanium has proven difficult due to its inherent properties; chemical reactivity, low thermal conductivity and a low modulus of elasticity all contribute to a poor machined finish [5]. These properties interact with the cutting tool, tungsten carbide, and degrade its life significantly resulting in premature fracturing. [6].

1.1.   Project Scope

The purpose of this paper is to investigate similarities and differences of machining commercially available titanium and 3D printed titanium. Even though compositionally they are the same, the manufacturing processes alters the materials properties changing the machinability. The motive behind conducting the investigation is to provide a solution to reduce the cost of manufacturing components from titanium alloys.

This will be accomplished by operating a lathe turning machine and performing numerous cutting passes using optimal machining parameters and investigating the difference in the swarf generated by different parameters, and wear rate of using different cutting tools. While quantifiable data is not easily generated, qualitative is suitable enough to express machinability. Characterisation of the swarf and cutting tools is done with a microhardness tester, optical microscope, scanning electron microscope (SEM) and then compositional analysis using an energy-dispersive x-ray spectroscope (EDS).

2. Literature Review

2.1. Titanium Ti-6Al-4V (Ti-64)

2.1.1. Introduction to Ti-64

Titanium Ti-6Al-4V is the most commonly produced grade of titanium containing around 6% aluminium, 4% vanadium, 90% titanium, and trace amounts of carbon, hydrogen, oxygen and iron as seen in Table 1 [7].

Ti-6Al-4V is used in industry due to its high strength to weight ratio, which is maintained at elevated temperatures; while being fracture and corrosion resistant. A comparison of specific strength favours titanium over steel at 288 $\frac{kN\,m}{kg}$ and 50 $\frac{kN\,m}{kg}$ respectively [7]. These characteristics make titanium sought after; unfortunately, due to the difficulty in machining processes, it does not make economic sense to use titanium unless its properties outweigh the overall costs.

Table 1 - Composition breakdown of Titanium Ti-64 [7].

Ti-6Al-4V	
C	<0.08%
Fe	<0.25%
N2	<0.05%
O2	<0.2%
Al	5.5-6.76%
V	3.5-4.5%
H2	<0.0125%
Ti	Balance

2.1.2. Difficulties with Machining Commercially Available Titanium

A quality machined finish is defined by the following three aspects: geometric accuracy, surface roughness and subsurface integrity [8]. To achieve a quality machined surface in titanium alloys, it is expensive, time consuming and problematic; the reasons are:

1. Titanium has a poor thermal conductivity. This means when machining, the heat is concentrated to the cutting tool (edge) and degrades the tool. The blunt tool then heats up the titanium, where it further impairs the machinability due to titanium remaining strong at elevated temperatures and low modulus of elasticity; See Figure 1 [5].
2. The alloying element within titanium alloy has a tendency to chemically react with the cutting tool. This weld creates a BUE on the cutting tool causing wear to the edge. Additionally, as the tool edge degrades, the more heat generated through ineffective chip removal; See Figure 2 [5].

3. During machining, titanium displays a plastic deformation which creates non uniform serrated chips. This is due to a low modulus of elasticity of titanium. The effect of this is an inaccurate geometry (inconsistent surface diameter and roughness) [5].
4. Serrated chips create fluctuations in the cutting force, creating an inconsistent surface geometry and roughness. This vibration creates a higher cutting temperature and premature tool degradation [2], [5].
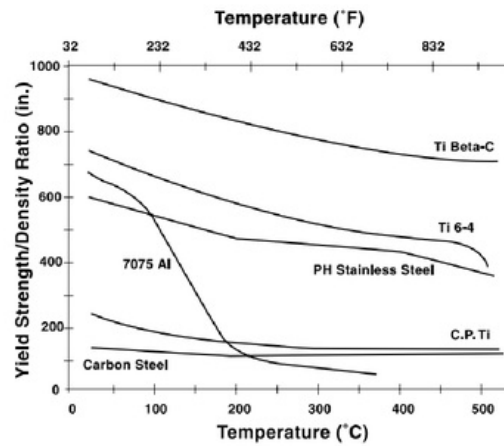
Figure 1 - Temperature of titanium, steels and aluminium at elevated temperatures [2].
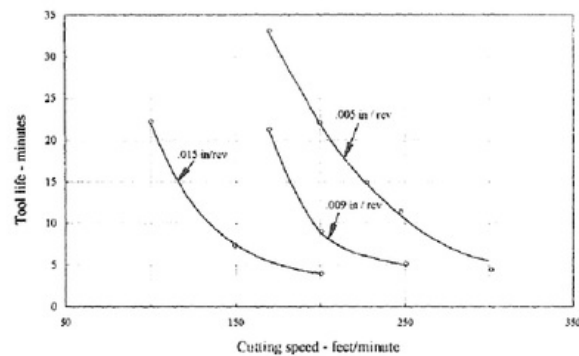
Figure 2 - Effect of cutting speed and feed on tool life in Ti-6Al-4V [2].

2.1.3. Metallurgy

2.1.3.1. Commercial-grade Ti-64

Ti-6Al-4V is a Grade 5 Alpha Beta alloy. Other grades of titanium alloys may be an alpha, near alpha, beta and near beta.

Alpha alloys are characterised by a hexagonal close packed crystalline structure, and is stable from room temperature to 882°C. Aluminium, is a single phase alpha stabiliser which when alloyed with titanium exhibits good weld-ability. The aluminium allows high strength and oxidation resistance, even at high temperatures (316-593°C). However, it cannot be heat treated as it is a single phase alloy. The alpha stabiliser raises the temperature the alloy will transform into a beta phase, also known as beta transus temperature [9].

Beta alloys are characterised by a body centred cubic structure, and is stable from 882-1688°C (melting point). Vanadium, a beta stabiliser, makes the alloy metastable and retains beta phase upon quenching and solution annealing. Beta stabilisers lower the beta transus temperature [9].

Alpha-beta alloys comprise of controlled amounts of both alpha and beta alloys. The result is a two phase system, which allows beta phase to exist below beta transus temperature. Beta stabilisers let the beta phase exist at room temperature; the higher content of stabilisers, the higher percentage of beta phase retained [9].

2.1.3.2. SLM 3D Printed Ti-64

Selective Laser Melting (SLM) is an additive manufacturing 3D printing process where a thin layer of metallic powder is spread across a bed so an overhead laser is able to melt the powder according to the specified program. The program is generated through CAD package software where the three dimensional part is sliced into 60µm 2D layers. The CAD software generates a .stl file which is read by all 3D printers. The printing chamber is filled with an inert gas, either argon or nitrogen to prevent porosity and contamination forming in the part being produced. After completion of each layer, another layer of metallic powder is spread and melted continuing until the part is completed [10].

The Ti-64 powder is of the same composition that is found in commercial Ti-64, however as they are different manufacturing processes, a different microstructure is produced. Due to the rapid heating then cooling of the powder/metal, a martensitic microstructure is formed. Martensite is a very hard crystalline structure and is formed when carbon does not have enough time to diffuse out of the crystalline structure, hence the material is supersaturated with carbon. [11].

2.2.   Built Up Edge

A built up edge (BUE) is defined as the welding of micro particles from the work-piece to the cutting tool. It is the main cause of tool failure. This BUE occurs at the rake face of the tool (see figure 3), and it continues to grow until reaching critical load and fracturing away, going between the tool and surface. As it is a hardened material, it compresses into the machined surface, resulting in premature tool wear, poor dimensional quality and surface finish [12, 13].

BUE are commonly generated under certain conditions: low cutting speed, high feed rates, Low rake angle, no cutting fluid, and large depth of cuts [14].
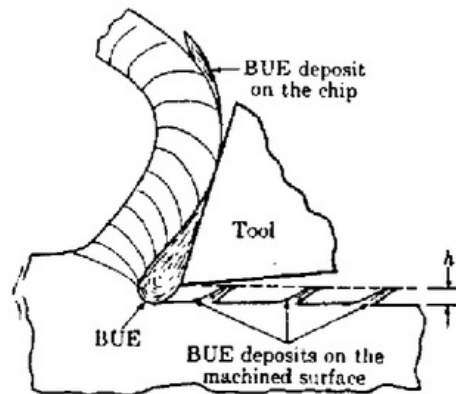
Figure 3 - Diagram of formation of BUE [41].
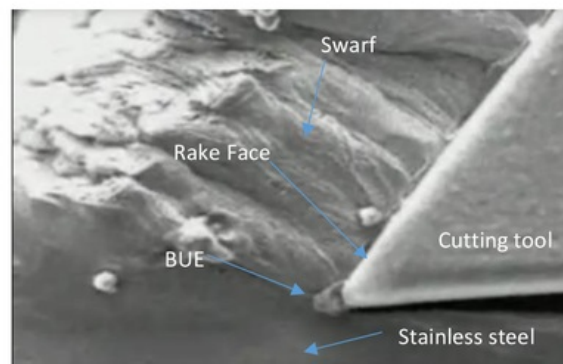
Figure 4 - Actual photo of Stainless steel being machined, and formation of a BUE is identified [6].

2.3.   Lathes

A lathe is a machine designed to rotate a work-piece between its central axis, where numerous cutting operations are performed to produce a symmetrical component. A metal turning lathe is used to turn metals and plastics to the desired shaped. Typical parts manufactured on lathes include: pistons, crankshafts and rims.

Lathes operate by rotating the work-piece in a chuck, which is mounted to the headstock. A carriage holds a cutting tool which cuts the work-piece to the operator's desired shape. The carriage is operated by two hand wheels denoting the X-Y axis. Additionally, a compound slide can be used to create angled cuts. A tailstock is a holder for drill bits, steadies, and other peripherals; it is aligned on the same axis as the headstock.

Safety is paramount when using a lathe. A lathe should not be operated unless the operator has received training in its function and safe working procedures. A cutting tool is removing material from a rotating mass. WorkSafe Vic describes the main hazards and common injuries, and provides a risk assessment. The major incidents are: entanglement of rotating parts, hit by chuck key or swarf and hit by work-piece [15].

To successfully produce a quality machined finish, the operator must machine the work-piece taking four parameters into consideration: cutting speed, feed speed, depth of cut and cutting tool material. This will be explained in greater detail in following sections.
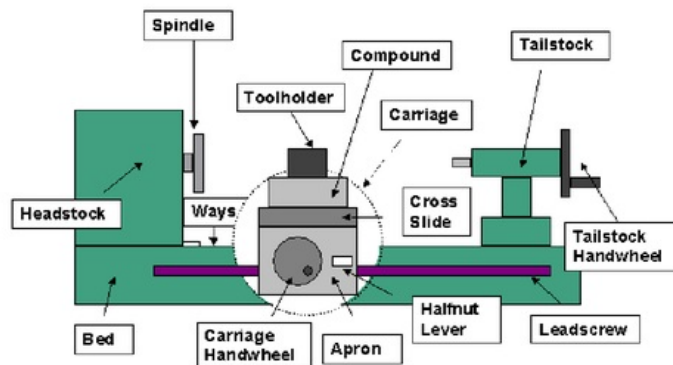
Figure 5 - A labelled diagram of all components that make up a lathe

2.4.   Cutting Tool Material

Advances in cutting tool technology have allowed the best possible finishes for every grade of steels and alloys to be produced. There are many characteristics that a cutting tool is categorised by. These are [5], [9]:

- High hot hardness to resist high stresses
- Good thermal conductivity
- Good chemical inertness

- Toughness and fatigue resistance
- High compressive, tensile and shear strength
- Wear resistance

The most common cutting tool materials can be divided into several groups:

High speed steels are the most common cutting tool used amongst hobbyists and light duty machinists. It has a hardness HRC 70. For titanium alloys it is recommended for milling, drilling and tapping applications. It is assumed unsuitable for this experiment [16].

Carbides are the most common cutting tool in industry. They are relatively affordable and have a longer life than high speed steels. Carbides are a composition of tungsten carbide and a cobalt binder. It has a hardness of HRC 90. These carbides can be coated to provide addition wear resistance. A chemical vapour deposition can produce a film of 50nm or various materials i.e. diamond, titanium [16].

Cubic boron nitride (CBN) is the second hardest material known upwards of HRC 95. It offered high resistance to abrasion at the expense of toughness. CBN is used for ferrous machining applications [16].

Polycrystalline Diamond (PCD) inserts are the hardest cutting tools available, however lacks fracture toughness. It is used only for non-ferrous. It has low chemical solubility in titanium to reduce diffusion, and mechanical strength and hardness to maintain integrity [17].

The cutting tool materials to be investigated is an uncoated and coated tungsten carbides. Both intended to cut titanium alloys

2.5. Machining Parameters

There are different opinions the machinability of Ti-64, which is hard to identify what to follow. RMI Titanium states it is similar to machining stainless steel, and Rahman *et al.* states it is problematic and to follow specific guidelines [5], [9]. Ideally, following a set of optimal machining parameters (OMP) would be used as its aim is to increase the life of the cutting tool. However, the topic of research is to investigate a BUE on a cutting tool, so OMP should not explicitly be follow. The machining parameters that should be looked at are the cutting speed, feed speed and depth of cut.

2.5.1. Cutting speed

The cutting speed (v) is the velocity between the cutting tool and the surface of the work-piece, measured in meters per minute. The greater the cutting speed, the more potential there is to remove more material when machining. The cutting speed is dependent on the material being machined, outer diameter of the workpiece and economic life of the cutter [18].

Cutting speeds vary between articles. Machinery's Handbook states an optimal cutting speed of 95ft/min or 29m/min and an average of 76m/min. The optimal cutting speed results in a lower tool

life, but better machined finish; Average refers to longer tool life, but poor finish [6] (see Table 3). Kahles *et al.* states a cutting speed of 9m/min [19], and Rahman *et al.* states 250m/min to 450m/min [5] (see Table 2). Suggestions of lower cutting speeds aims to get a better machined finish.

Since cutting tools have numerous cutting faces, the possibility to use an optimal and average cutting speed is viable. Hence, a cutting speed of 29m/min and 76m/min is used.

Table 2 - Typical parameters for machining Ti-6Al-4V [19]

Operation	Tool materials	Cutting speed (in./min)	Feed rate	Depth of cut (in.)
Turning (rough)	C-2	150	0.010 in./rev.	0.250
Turning (finish)	C-2	200	0.006–0.008 in./rev.	0.010–0.030
Turning (finish)	C-2	300	0.004–0.008 in./rev.	0.010–0.030
End mill (⅛–1″ dia.)	M42 HSS	60	0.003 in./tooth	0.125″
End mill (⅛–1″ dia.)	C-10	200	0.005 in./tooth	0.150–0.200″
Drill (⅛–½″ dia.)	M42 HSS	30	0.005 in./rev.	
Drill (⅛–½″ dia.)	C-2	40	0.004 in./rev.	
Ream	M42 HSS	20	0.010 in./rev.	
Ream	C-2	35	0.010 in./rev.	
Tap	M7 HSS	15	—	
Broach	M3 HSS	12	0.003 in./tooth max.	
Spline shape	M42 HSS	12	0.012 in.²/stroke	

Table 3 - Machinery's Handbook cutting feeds and speed for tuning Titanium alloys [6].

Material		Brinell Hardness	HSS Speed (fpm)	Uncoated Carbide (Tough) f = feed (0.001 in./rev), s = speed (ft/min)	
				Opt.	Avg.
Commercially Pure and Low Alloyed					
99.5Ti, 99.5Ti-0.15Pd		110–150	100–105	f 28 / s 55	13 / 190
99.1Ti, 99.2Ti, 99.2Ti-0.15Pd, 98.9Ti-0.8Ni-0.3Mo		180–240	85–90	f 28 / s 50	13 / 170
99.0 Ti		250–275	70	f 20 / s 75	10 / 210
Alpha Alloys and Alpha-Beta Alloys					
5Al-2.5Sn, 8Mn, 2Al-11Sn-5Zr-1Mo, 4Al-3Mo-1V, 5Al-6Sn-2Zr-1Mo, 6Al-2Sn-4Zr-2Mo, 6Al-2Sn-4Zr-6Mo, 6Al-2Sn-4Zr-2Mo-0.25Si		300–350	50		
6Al-4V		310–350	40		
6Al-6V-2Sn, Al-4Mo,		320–370	30	f 17	8
8V-5Fe-1Al		320–380	20	s 95	250

2.5.2. Feed Speed

The feed speed (f) is the relative velocity that the cutter advances along the work-piece, measured in millimetres/revolution. Generally, the slower the feed speed, the better the surface finish is. The feed speed is dependent on type of tool, surface finish desired, power available, strength of work-piece, machinability of the material being cut [9].

Similarly, the feed speed is different from all articles, but both the optimal and average feed speeds can be used respectively with cutting speeds. High feed rates are suggested. Machinery's Handbook suggests an optimal and average feed rate of 0.431mm/rev and 0.203mm/rev respectively (see Table 3) [6]. Similarly, Kahles *et al.* states 0.203mm/min (see Table 2) [19].

2.5.3. Depth of Cut

Depth of cut (DoC) refers to how deep the tool cuts into the work-piece. General practice is to use a depth of cut five times the feed rate. Larger DoC removes material quicker at the expense of a shorter tool life, as the cutting edge has to withstand the force and heat of removing a large amount of material [5], [6].

Calculation of cutting and feed speed with DoC returns a material removal rate; this can also determine the cutting life of the tool [6]. Rahman *et al.* and Kahles *et al.* both state a DoC of 0.05mm (see Table 2) [5] [19].

2.5.4. Additional Processes

Numerous articles suggest combatting titanium's low thermal conductivity which hinders its ability to dissipate heat by using copious amounts of cutting fluid. Cutting fluid acts as a coolant and a medium to carry swarf away. This minimises the BUE generated on the cutting tool. Consequently, cutting fluid is not used as it will hinder the ability to recreate a BUE.

2.6.   Hypothesis & Expected Outcome

Hypothesis

- The hypothesis is that as 3D printed Ti-64 is a harder material that contains martensite, it will be harder to machine.

- The wear of the carbides is dependent on the type used, as most carbides are designed for specific operations and materials. So any cutting tool designed to cut titanium will perform well.

- Using optimal machining parameters will cause the tungsten to chip out as it is a high feed rate for the respective spindle speed.

Previous research

Rahman *et al.* [5] conducted similar experiments around the composition of a BUE. However, the findings lack depth. Rahman *et al.* describes the interaction between titanium and a polycrystalline diamond (PCD), binder-less cubic boron nitride (BCBN) and cubic boron nitride (CBN) cutting tools.

It stated that poor life of the cutting tools was due to diffusion of the binder. The BCBN insert saw no diffusion, due to having no binder, resulting in longer life. The PCD insert saw diffusion of the binder material, cobalt and carbon found in the swarf; similarly, the CBN insert saw diffusion of cobalt, then boron diffusing-dissolving [5]. These results were found using high speed machining parameters - speed: 400m/min; feed: 0.05mm/tooth; depth of cut: 0.05mm]. It does not consider results of using

tungsten carbides, which is to be investigated. However, previous research will still be used to compare with experimental findings.

There is currently no scientific journals or papers on the machinability of SLM 3D printed Titanium 6Al-4V

Expected outcome

- 3D printed will be poor to machine, fractured carbides. Material won't be homogenous, voids expected in the bar.

- Commercial Ti-64 will machine nicely provided a fresh tip is used. Similar to machining stainless steel.

- Coated carbide will suffer coating failure.

- Uncoated carbide will suffer tool fracturing – especially machining 3D Printed Ti-64.

- A large BUE will form on both carbides used.

3. Experimental Procedures

3.1. Sample Preparation

3.1.1. Machining Preparation

The samples to be examined are an uncoated and coated tungsten carbides. These have several cutting edges all of which are subjected to different machining parameters. The machining parameters are based on an average and optimal range, which aim to improve surface finish at expense of tool life and vice-versa.

All machine work will be contracted to Macquarie Engineering & Technical Services (METS). Specifications of all machining operations is documented into a job sheet for a quote and estimated time of completion.

Preparation of the sample is processed at METS. Cleanliness is generally not a concern in machine shops, however to ensure no contamination occurs, a liberal clean down of the lathe turning machine is required. Typically, a lathe is quite oily; The machine ways, chuck, hand-wheels, and other components get oiled regularly to keep 'clean' and free from oxidisation or as over spray from previous machining jobs. Oily components are not ideal, so minimisation of oil around the specimen ensures characterisation is as accurate as possible with no concerns for errors.

The workpieces will be affixed to the lathe using a 3 jaw chuck. It automatically centers the workpieces. A stickout of at least half the length of the workpieces is required. The dimensions of the commerical grade Ti-64 bar is 38.1mm OD x 150mm. The 3D printed Ti-64 is smaller at 10.8mm OD x 78mm. So a stickout of 75mm and 39mm should be used. Using half the length of the material aims to prevent deflection during machining. Having two halves to the materials allows each half to be used specifically for different machining parameters and different cutting tools.

The carbides are fixed to the tool post where passes are repeatedly done until the tool is blunt. A chip tray is placed underneath the rotating chuck to collect the swarf after each test. The tool is to do passes at a specified machining parameter as specified in Table 4.

Table 4 - Machining parameters used on Titanium Bar

Specimen	Specimen Diameter (mm)	Feed (mm/rev)	Speed (m/min)	RPM	DOC (mm)
Commercial Titanium Optimal	38.1	0.431	29	242	0.05
Commercial Titanium Average	38.1	0.203	76	635	0.05
3D Printed Titanium Optimal	10.8	0.431	29	855	0.05
3D Printed Titanium Average	10.8	0.203	76	2240	0.05

The spindle speed, useful for the lathe operator is calculated by the cutting speed seen in Table 4. The formula is given by:

$$n = \frac{V_C \times 1000}{\pi \times D_m} \; [20]$$ *Equation 1 - Lathe spindle RPM*

Where:

n is the Spindle speed (rpm); Vc is the Cutting speed (m/min); Dm is machined diameter (mm)

$$n_{t1} = \frac{29 \times 1000}{\pi \times 38}$$

$$n_{t1} = 242 \; rpm$$

After all machining operations, the cutting tools and swarf are characterised and results are formed. Care should be taken to ensure the carbides and swarf are logged for which machining parameters it was tested with.

3.1.2. Hardness Testing

Hardness testing required several steps of preparation before testing, mounting and polishing.

The mounting of the specimen is performed in a Struers Citopress 10. It is a hot mounting press that melts a thermosetting Bakelite to surround the specimens so polishing can be performed. The Bakelite medium used is Polyfast, which uses a carbon based filler so SEM analysis can be performed on the specimen.

The mounting procedure is performed in 5 minutes; 3 minutes at 250 bar and 150°C is spent heating and 2 minutes at atmospheric pressure spent cooling. After being released from the Citopress, it can be washed and cleaned and is ready for polishing.

Polishing is a 3 step process broken down into grinding, polishing and lapping (in order of intensity). The polishing was performed on a Struers Tegramin 25 polisher. The information for time, force, abrasive and surface is from Struers e-Metalog [21]. Care must be taken between all steps to ensure no contamination from the previous polishing step otherwise scratching will occur. Figure 9 displays the finished product.

Table 5 - Polishing method used to bring titanium up to a high polish ready for hardness testing.

STEP	SURFACE	ABRASIVE	SPEED (RPM)	TIME (MIN)	FORCE (N)
GRINDING	Mezzo220 220G diamond grinding disc	N/A	300	1:00	40
POLISHING	Largo Composite fine grinding disc	Diamond 9μm	150	4:00	30
LAPPING	Chem Porous Neoprene lapping disc	OP-S 0.04μm	150	5:00	30

24

3.2.   Characterisation

Characterisation is the process of determining a materials structure, properties and composition. Two methods of characterisation are used to understand the interaction between titanium and cutting tools. A Scanning Electron Microscope (SEM) and Energy-Dispersive X-Ray Spectroscopy (EDS), which are usually combined together, are used to determine the shape and composition respectively.

3.2.1. Scanning Electron Microscope

A Scanning Electron Microscope (SEM) relies on focusing an electron beam to generate an image of a sample. The electron beam uses detectors to collect information about a specific area where an interaction between electrons and atoms happens [22]. A SEM is also able to create topographical maps of the surface, useful for examining the surface roughness.

The SEM is used to photograph the cutting edge of the cutting tool. The image is used to determine whether there is any chemical contamination or weld interaction between the titanium and cutting tool. Any premature wearing of the tool can also be examined. Additionally, the swarf chips from machining can be examined; the shape of the chip tells how the material was cut and its effectiveness.

3.2.2. Energy-Dispersive X-Ray Spectroscopy

An Energy-Dispersive X-Ray (EDS) is commonly bundled with a SEM. It's a non-destructive analytical device that requires very little sample preparation; Cleanliness is important as any trace amounts of impurities will show under analysis and can alter results. It provides a quantitative and qualitative analysis of the chemical composition of the sample. The electron beam used from the SEM charges the atoms of the samples. This excites the atoms, and goes into a higher energy state, where they return shortly to a lower energy state. The energy difference between higher and lower energy state is released in the form of an X-Ray. An energy dispersive spectrometer detects these X-Rays and generates a spectrum displaying a series of energy levels, measured in electron voltage (eV). This is displayed in a graph displaying the type of element and the atomic-percentage (wt. %) [23].

An EDS will plot the chemical composition of the cutting tools and display the wt. %. Comparing initial results (before machining) and then after machining will inform whether there is a difference in composition. Additionally, comparing the swarf chips after machining and comparing with raw Ti-64 will determine if there is any diffusion from the cutting tools.

3.2.3. Hardness Testing Vickers

A Vickers hardness tester is a microhardness tester which uses a diamond with 136° opposing angle faces (a square pyramid).The diamond imprints the specimen using a load specified by the user. The indent created is measured by an optical measurement system which measures the parallels of the indentation, converting that into a figure, also dependent on the load used. Hardness testing must be done on a polished surface so the optical system can detect the imprint. Following the sample preparation from section 3.1.1. is required.

The Struers Durascan requires very little setup and operational knowledge. Given the load, the machine will automatically perform the hardness test and produce a result. A load of 5kg for titanium alloys is advised.

A matrix pattern of hardness testing is recommended to check the consistency of hardness along an x-y axis. It is not specified how many hardness tests are required before the average can be taken and a final result can be produced, however any more than 5 tests is generally acceptable.

3.3.   Experimental Procedure

1. Mount commercial grade Ti-64 bar in lathe. Set up lathe with a NEW Tungsten carbide insert.
2. Take 1 machining pass using the following OPTIMAL machining parameters:
   - Speed: 29   m/min
   - RPM: 242
   - Feed: 0.431   mm/rev
   - DoC: 0.05   mm

   Collect the swarf shavings produced, bag and label contents.
3. Under an optical microscope, investigate if any wear is present. If so, continue to step 5. If not continue to step 4.
4. Using the same cutting edge on the carbide insert, complete another machining pass (follow step 2).
5. Record the required amount of machining passes needed to observe any wear (P1). This becomes the baseline for OPTIMAL machining. Record which edge was used, and list any observations about wear. This edge is ready for characterisation. Collect the swarf shavings produced, bag and label contents.
6. Using a different edge of the same tungsten carbide cutting insert, take 1 machining pass using the following AVERAGE machining parameters:
   - Speed: 76   m/min
   - RPM: 635
   - Feed: 203   mm/rev
   - DoC: 0.05   mm
7. Repeat steps 3-5, however using all AVERAGE machining parameters.

This now becomes the baseline for the proceeding machining - The required number of machining passes and DOC. *At this stage the baseline for proceeding machining is*

established. So every other sample of Ti-64 will be machined using these same parameters. The wear rate, machinability, and BUE will be compared between OPTIMAL & AVERAGE, and different microstructures.

8. Using a different coated tungsten carbide insert, complete the same experiment using the baseline machining parameters, using a different cutting edge for both operations.

I.e. OPTIMAL:

- Speed: 29   m/min
- Feed: 431   mm/rev
- DoC: 0.05   mm
  Passes: P1 (recorded from step 5)

AVERAGE
- Speed: 76   m/min
- Feed: 203   mm/rev
- DoC: 0.05   mm
- Passes: P1 (recorded from step 5)

At this stage, the machining for commercial Ti-64 is completed. The commercial Ti-64 bar can be removed and is now ready for machining with the SLM 3D Printed bar.

9. Mount SLM 3D Printed Ti-64 bar in lathe. Set up lathe with the same tungsten carbide used in step 1.

10. Since the 3D Ti-64 workpiece has half the amount of stick out, perform twice the amount of passes noted down in P1. Perform OPTIMAL machining parameters
    - Speed: 29   m/min
    - RPM: 855
    - Feed: 0.431   mm/rev
    - DoC: 0.05   mm
    Collect the swarf shavings produced on the first and last machining pass; bag and label contents.

11. Similarly, perform twice the amount of passes P1 using AVERAGE machining parameters.
    - Speed: 76   m/min
    - RPM: 2240
    - Feed: 203   mm/rev
    - DoC: 0.05   mm
    Collect the swarf shavings produced on the first and last machining pass; bag and label contents.

12. Using the same carbide used in step 8, repeat steps 10-11.

4. Results and Discussion

The results collected with the SEM and EDS all followed the same strict handling procedures. After the machining procedures were completed, they were thoroughly cleaned with acetone. The solvent removed any oils, detergents and dirt from the surface necessary for analysis. Any handling after the solvent cleaning needs to be performed using surgical gloves. This is to prevent the contamination from hands, oils and/or sweat, from entering the vacuum sealed SEM. If contamination is present, it will hold onto the electron beam charge and illuminate as white; any organic material will act this way. All SEM work was performed by an experienced operator, Nadia Suarez-Bosche.

4.1.   Comparison of Titanium-64 Material

4.1.1. Results

Figure 6 displays a backscattered image of a highly polished commercial grade Ti-64 specimen. The imaging shows the microstructure of the alloy; the dark areas are alpha phase and the lighter areas are the beta phase. The numbered boxes refer to EDS area analysis point.
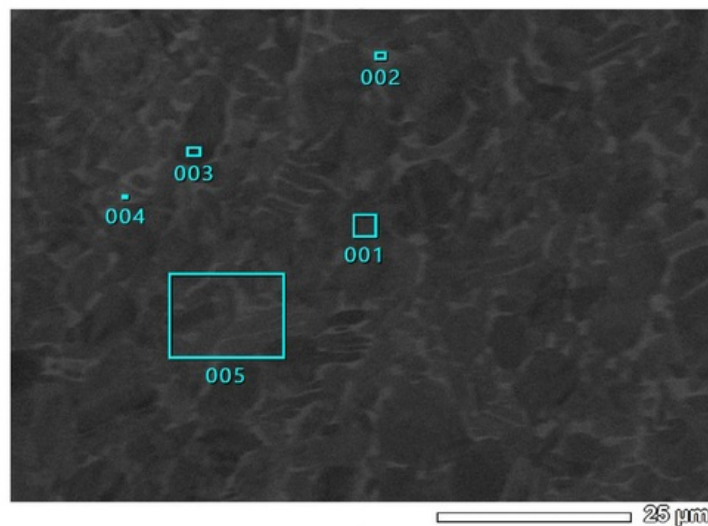

Figure 6 - EDS area analysis map of commercially available Ti-64.

28

Figure 7 displays a backscattered image of a highly polished SLM 3D printed Ti-64 sample. The microstructure seen is martensite. This forms during the manufacturing process as the laser solidifies the metallic powder for microseconds, before being rapidly cooled.
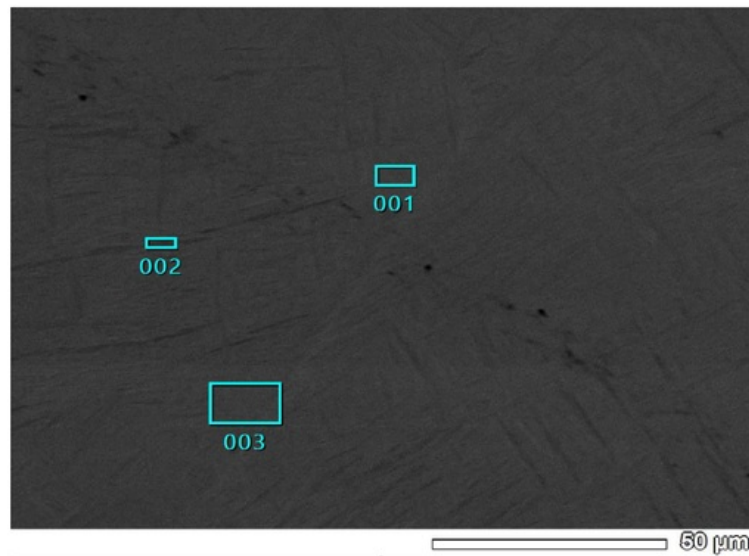
Figure 7 - EDS area analysis map of SLM 3D Printed Ti-64.

Table 6 describes the composition data from completing EDS analysis on specimens of commercial grade and SLM 3D printed Ti-64. The numbers in the table refer to areas seen in Figure 6 and Figure 7 shown above. The certified commercial Ti-64 is the inspection certificate that came with the purchase commercial Ti-64 bar. The results from certified should match measured commercial.

Table 6 - Compositional analysis table comparing different manufactured Ti-64

Element	Measured Commercial Ti-64					Certified Commercial Ti-64	SLM 3D Printed Ti-64		
	1	2	3	4	5		1	2	3
Carbon	1.26	1.44	1.22	1.41	1.32	0.016	1.21	1.19	0.97
Aluminium	6.79	3.34	5.46	4.47	5.65	6.2	5.69	5.74	5.86
Titanium	90.15	79.75	87.46	84.16	88.67	88.79	88.72	88.68	90.34
Vanadium	1.66	15.47	5.64	9.72	4.36	4.26	4.02	4.39	2.79

Figure 8 shows the difference in hardness between commercial grade and SLM 3D printed Ti-64. The results was calculated by taking numerous measurements of hardness along pieces of highly polished Ti-64.
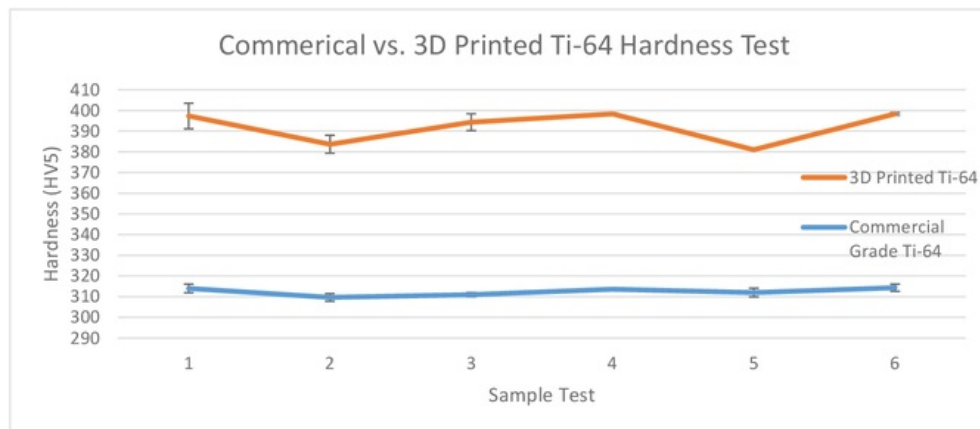

Figure 8 - Graph comparing hardness of commercial and 3d Printed Ti-64.

4.1.2. Discussion

4.1.2.1.   Sample Preparation

The specimen preparation involved attaining a small piece of both materials and mounting and polishing with the Struers CitoPress and Tegramin exactly as outlined in section 3.1.2. See Figure 9 for the prepared specimen. Polyfast Bakelite was used for mounting as it is conductive for SEM/EDS analysis. The polished surface unknowingly led to focusing difficulties with the SEM. An etchant should have been used to produce a greater contrast between the grain structures and would have ultimately resulted in a clearer focused image, and possibly more accurate EDS analysis. This is not strictly important as there are previously published papers and data on the microstructure of commercial grade and SLM 3d Printed Ti-64.

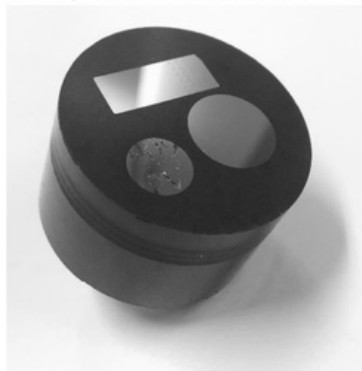The specimens used for SEM/EDS analysis was also used for hardness testing.

Figure 9 - Ti-64 specimens mounts and polished in Polyfast Bakelite puck.

4.1.2.2. Composition Analysis

The materials used for the overall experiment, commercial grade and SLM 3D printed Ti-64, were first subjected to compositional analysis to confirm their properties with published and supplied data. Ideally both commercially available and 3D printed Ti-64 should have the same composition, however different manufacturing techniques can introduce differences.

Table 6 displays the difference in composition of measured titanium. The 3D printed Ti-64 specimen has far more consistent values than commercial grade. This is primarily due to the manufacturing process, as instead of smelting a combination of metals together, a metallic powder is used. As the powder is almost completely homogenous, when it is welded together by laser, the composition stays the same as the powder. The microstructure formed is martensite, which is much harder than alpha and beta phase particles; hence, the 3d printed parts are harder than commercial titanium. This is confirmed in section 4.1.2.3. Visually, martensite forms as an arrangement of straight lines ceasing by another group of straight lines, normally at a different angles. The microstructure presented in Figure 7 displays a perpendicular cross hatching. The perpendicular forming is due to the manufacturing process as the laser melting the powder operates in an overlapping lattice pattern, which is easier and simpler to program and operate as fewer coordinates are required.

The commercial Ti-64 bar was purchased with an inspection certificate stating the composition (Figure 44). Analysis was still done on the specimen to confirm its composition and EDS is working. Tested area number 5, see Figure 6, is an overview measurement of the specimen and resulted in the closest values out of the five tested to the certificate. Titanium and vanadium are within 1% and 3% respectively of the certificate, while carbon and Aluminium are 99% and 9% away. The high value for carbon may be due to the medium holding the titanium samples, as it is a carbon based thermosetting plastic. The carbon in the plastic allows it to be conductive, necessary for SEM and EDS analysis. While the specimen was cleaned with ethanol before, possible contamination or interference from the carbon based plastic may have altered the results.

Areas 1 -4 are positioned to measure specific points of the metal in attempt to measure the values of the alpha and beta phases. While the values for the alpha and beta phase are not consistent in weight%, they are consistent with literacy. Area 1 and 3 both look at the alpha phase, and 2 and 4 look at the beta phases. Alpha phase has larger amounts of aluminium, as aluminium acts as a stabiliser, and Beta phase generally has high amounts of vanadium, where similarly, vanadium is the stabiliser for beta phase. The carbon content has consistent values for both the alpha and beta phases.

4.1.2.3. Hardness Testing

Hardness testing was performed on a highly polished piece of both commercial grade and 3D printed Ti-64. The comparison allowed an insight into how machining the materials may be. Generally, the harder the material the faster the cutting tool wears out, and the geometry and roughness of the workpiece worsens.

A Struers Vickers hardness tester was used to determine the hardness of the specimens. A test was performed on each specimen 18 times 1mm apart from one another in a 6 x 3 matrix. This was to check the consistency of hardness and also to get an average hardness for the metal. Each test was performed using a 5kg load. See Table 9 and Table 10 in Appendix for tabulated data. Additionally, see Figure 42 and Figure 43 to see the result of the hardness test for commercial and 3D printed Ti-64 respectively.

Figure 8 displays the results of hardness testing. The sample test number refers to a series of tests performed along a single line.

3D Printed Ti-64 has an average hardness of 392HV5, with a range of 28. While the 3D printed Ti-64 has a much higher hardness, its inconsistency explains suggests it is difficult to machine. Machining is expected to be harder as the carbide will be subjected to titanium of different structures and hardness' causing a vibration reducing the cutting action and decreasing the surface finish. The metal's hardness is directly related to the microstructure.

Commercial Ti-64 has an average hardness of 312HV5. The range of results was 9. This shows the commercial Ti-64 is very consistent. A consistent hardness means machining is easier as the force required by the carbide to cut is lower but more consistent.

4.2. Comparison of Carbide Cutting Tools
4.2.1. Results

Figure 10 displays the EDS analysis map for a new DNMG carbide, used as a reference. EDS analysis confirms that the carbide has a titanium carbo-nitride coating. Area 001 and 003 shows a 73 wt. % of titanium with the balance being nitrogen, oxygen and carbon. No tungsten is present, confirming that the whole tungsten is coated. See Table 12 for tabulated EDS data.
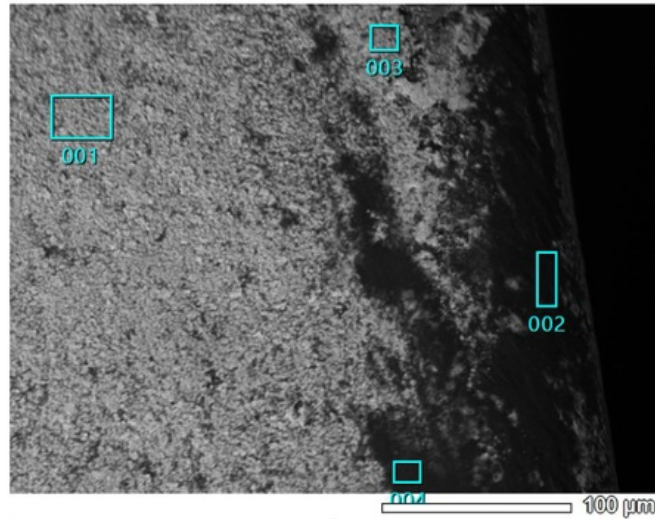

Figure 10 - Reference edge for DNMG.

Figure 11 shows the EDS analysis map for a TNNG tungsten. This is specified as an uncoated carbide, as confirmed by areas 004 and 005 showing a wt. % of 90 with the balance being carbon. Areas 001-003 came up as being predominantly carbon with trace (<10%) elements tungsten. Note area 003 which has the edge worn away. See Table 12 for tabulated EDS data.
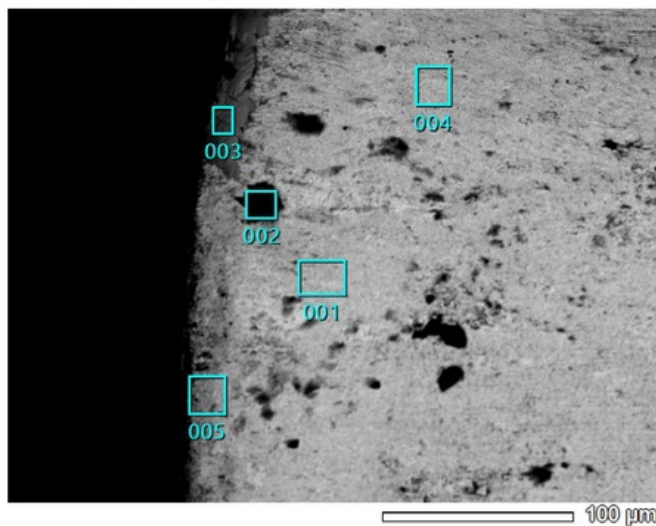

Figure 11 - Reference edge for TNNG.

33

Figure 12 displays the EDS analysis map for a DNMG carbide after machining 8 passes of commercial grade Ti-64 using Optimal machining parameters. When comparing to the reference edge, an increase of carbon is present, additionally showing signs of aluminium (area 002). The possibility that diffusion or a BUE occurred in area 006, as 5% and 3.5% of aluminium and vanadium respectively are present. See Table 13 for tabulated EDS data.
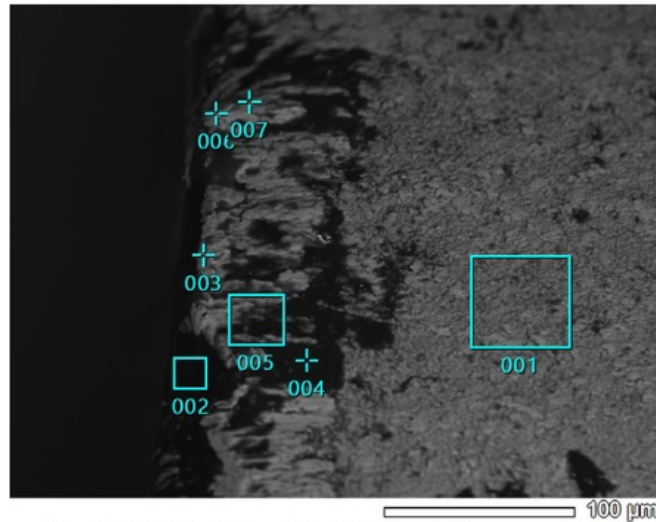

Figure 12 - DNMG cutting tool after Optimal machining commercial Ti-64.

Figure 13 displays the EDS analysis map for a DNMG carbide after machining 8 passes of commercial grade Ti-64 using Average machining parameters. The parting line that can be seen running through area 013 was tested and denied any coating failure. Area 008 displays a composition similar to that of commercial grade Ti-64. Similarly area 009 shows signs of Ti-64, but with larger quantities of carbon, oxygen and nitrogen 10%, 8.5% and 22% respectively. Area 011 and 012 are spots of carbon. See Table 13 for tabulated EDS data.
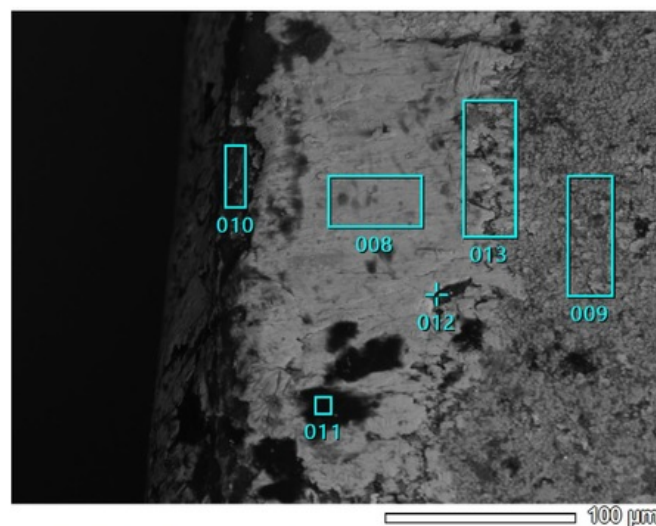

Figure 13 - DNMG cutting tool after Average machining commercial Ti-64.

34

Figure 14 displays the EDS analysis map for a TNNG carbide after machining 8 passes of commercial grade Ti-64 using Optimal machining parameters. The dark line running through the middle was analysed as impurities – carbon and oxygen. Areas 002 and 006 showed around 45wt% of titanium and 3wt% of aluminium, caused by a BUE. See Table 14 for tabulated EDS data.
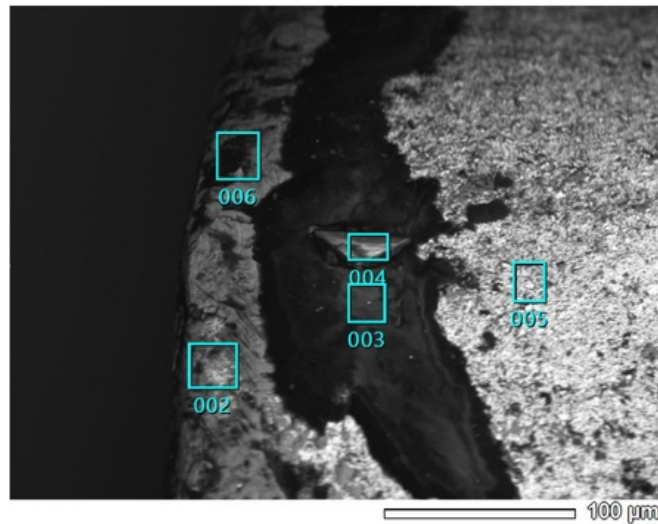

Figure 14 - TNNG cutting tool after Optimal machining commercial Ti-64.

Figure 15 displays the EDS analysis map for a TNNG carbide after machining 8 passes of commercial grade Ti-64 using Average machining parameters. Area 006 confirms 70wt% of tungsten with remainder being carbon. Interestingly, areas 001, 003, 005 all wt% the same of Ti-64, with no tungsten present. Area 002 is a deposit of carbon. See Table 14 for tabulated EDS data.
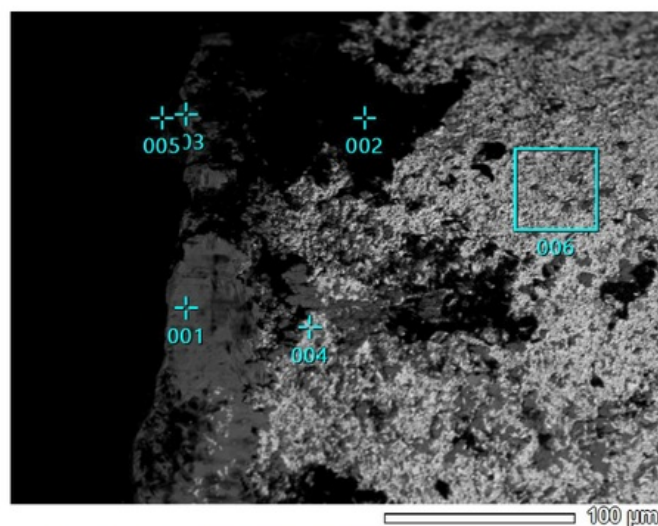

Figure 15 - TNNG cutting tool after Average machining commercial Ti-64.

Figure 16 displays the EDS analysis map for a DNMG carbide after machining 8 passes of SLM 3D printed Ti-64 using Optimal machining parameters. The coating of the carbide failed in area 002 as the tungsten content is at 40wt%; remnants of the coating are present with 22wt% present in the same area. Area 003 and 004 still has the coating, with no traces of tungsten, however show 3wt% of vanadium suggesting BUE or diffusion from the titanium. Area one is identified as carbon with traces of titanium, oxygen, and nitrogen. See Table 15 for tabulated EDS data.
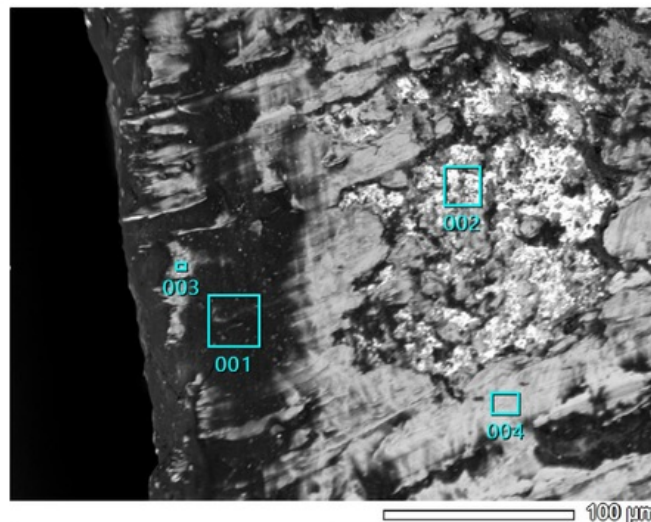

Figure 16 - DNMG cutting tool after Optimal machining 3D printed Ti-64.

Figure 17 displays the EDS analysis map for a DNMG carbide after machining 8 passes of SLM 3D printed Ti-64 using Average machining parameters. Area 002 and 004 shows Ti-64 present, containing 82wt% titanium, 5.2wt% aluminium and 3.3wt% vanadium, this is caused by diffusion or a BUE. Area 1 contains lots of impurities, but also has 35wt% of aluminium and 7wt% titanium. Area 003 and 005 are areas of mainly carbon 50wt%, with oxygen and nitrogen. The coating is still intact as no tungsten is present. See Table 15 for tabulated EDS data.
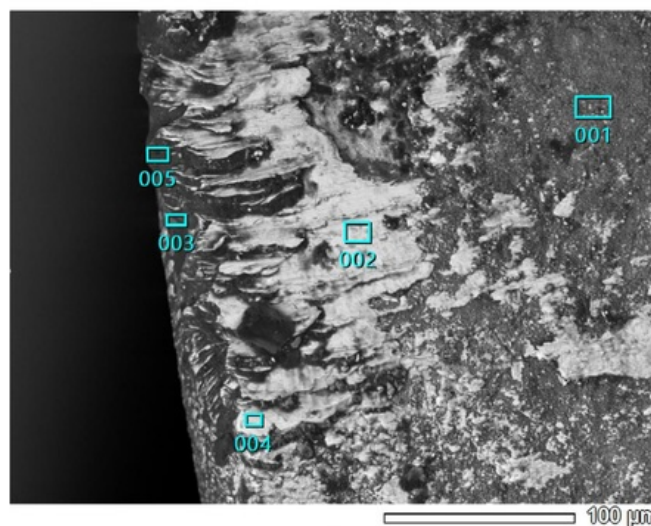

Figure 17 - DNMG cutting tool after Average machining 3D printed Ti-64.

36

Figure 18 displays the EDS analysis map for a TNNG carbide after machining 8 passes of SLM 3D printed Ti-64 using Optimal machining parameters. Area 001 confirms that tungsten is still present at 82wt%. Area 002, 004, 005 and 006 confirm the dark grey glob and similarly coloured spots, are a BUE of Ti-64 material. Area 003 is a build-up of carbon. See Table 16 for tabulated EDS data.
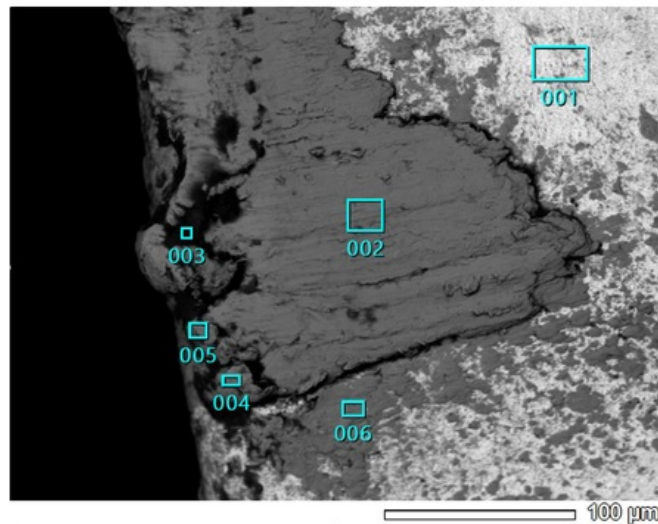
Figure 18 - TNNG cutting tool after Optimal machining 3D printed Ti-64.

Figure 19 displays the EDS analysis map for a TNNG carbide after machining 8 passes of SLM 3D printed Ti-64 using Average machining parameters. The image shows a BUE of Ti-64 on the tungsten. 003 confirms the tungsten underneath; 002 and 004 confirm the presence of Ti-64 metal. 001 shows the presence of carbon attached to the Ti-64 BUE. See Table 16 for tabulated EDS data.
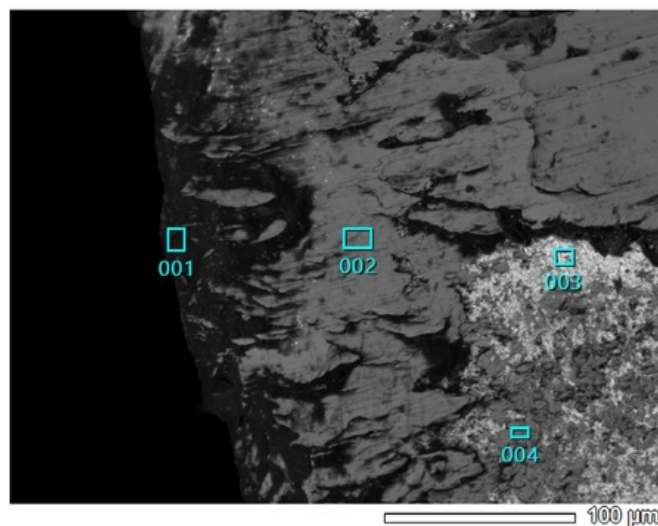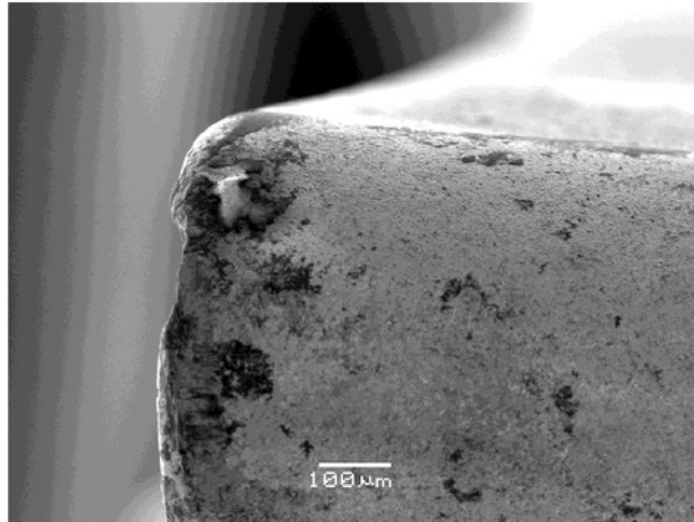

Figure 19 - TNNG cutting tool after Average machining 3D printed Ti-64.

37

Figure 20 displays the tool failure that occurred on an uncoated TNNG carbide. The cutting edge of the carbide has completely chip away.

Figure 20 - Tool edge failure of a TNNG carbide machining optimal commercial Ti-64.

4.1.1. Discussion

4.2.1.1. Sample Preparation

The cutting tools use to complete the machining is:

1. Sandvik DNMG 11 04 04-PM 4225
2. Kyocera TNNG 331TK SW05

The DNMG (Figure 21) has a medium temperature chemical vapour deposition (MTCVD) titanium carbo-nitride (TiCN) coating, designed as a semi finishing cutting tool for steel and steel castings. The carbide is designed as a universal tool, able to handle continuous and interrupted cuts at high material removal rates [24].

The TNNG (Figure 22) is designed as a medium roughing cutting tool for machining titanium alloys. It is uncoated, with a polished chip breaker, designed for smooth chip control with less adhesion. The carbide has a composition of tungsten cobalt [25].

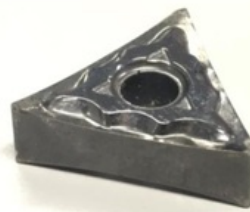Figure 21 - An image of Sandvik DNMG 11 04 04-PM carbide cutting tool.

Figure 22 - An image of the Kyocera TNNG carbide cutting tool.

The machining of the titanium was outsourced to Macquarie Engineering Technical Services (METS). The workpiece was set up in a Harrison M500 lathe, and hand indicated true. The 3D printed specimens required an initial clean-up cut as the surface is very rough. As it is a geared lathe, with an AC induction motor, there are pre-set spindle speeds. With only a selection to choose from, at times the surface speed had to be adjusted. As the optimal is designed as the most efficient material removal parameter, and average or surface finish, the speeds chosen were respective with their purpose. For example, the RPM for average was increased to the next closes pre-set speed.

Table 7 - Describes the machining parameters desired, however due to lathe constraints, alterations had to be made.

	Commercial Ti-64				3D Printed Ti-64			
	Optimal		Average		Optimal		Average	
	Desired	Actual	Desired	Actual	Desired	Actual	Desired	Actual
Speed (m/min)	29	28	76	92	29	27	76	68
RPM	242	235	635	770	855	800	2240	2000
Feed (mm/Rev)	0.431	0.4	0.203	0.2	0.431	0.4	0.203	0.2
DoC	0.05	0.05	0.05	0.05	0.05	0.05	0.05	0.05

As the depth of cut is determined by the machining operator, this value remained consistent. A digital readout helped to maintain the depth of cut at 0.05mm for all machining passes.

Machining proceeded by taking a first pass with the Sandvik DNMG tungsten. As it is not specifically made for machining titanium, it was used as the control to measure required number of machining passes. After the first pass was completed, an optical microscope was used to determine the wear rate or any build up edges occurring. It took 8 machining passes until a noticeable wear began to show, see Figure 23. Notice the BUE occurring on the edge, overhanging the coating.
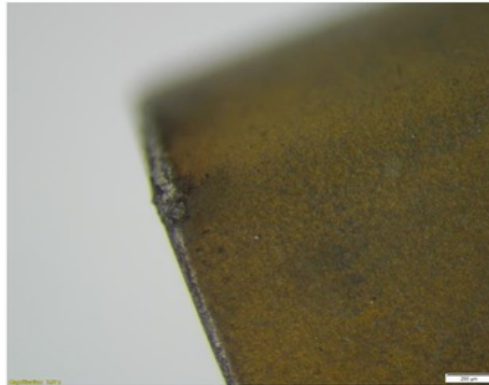

Figure 23 - Sandvik DNMG tungsten after 8 machining passes.

Since the commercial and 3D printed Ti-64 bar had a stick out of 76mm and 38mm respectively, the commercial received 8 machining passes, and 3D printed received 16 machining passes. The RPM for each material was adjusted, see Table 7, so that each carbide is removing the same amount of material for both specimens.

Characterisation for the carbides required a special way to hold them at just the right angle, as the cutting action of the carbide tools is not on the exact point of the tool, but rather to the right of the edge, still on the radius of the point. The SEM/EDS requires the inspected surface to be directly facing up. A small aluminium screw vice, Figure 24, was used. This helped positioning the carbides in the correct orientation. As the vice was in direct contact with the carbides, EDS analysis was completed to check the composition, in case any contamination radiating to the carbides occurred. This analysis can be seen in the appendix, see section 8.2.
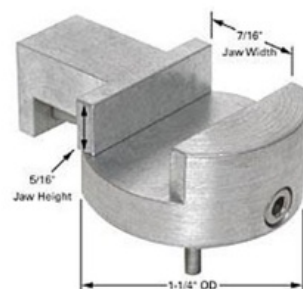

Figure 24 - Small aluminium screw vice used to mount the carbides for SEM and EDS analysis.

40

4.2.1.2.   Wear and BUE

No quantifiable measure of the wear was able to be gained, due to not having the analysis techniques available; only visual qualitative comparisons were made.

Figure 20 shows the cutting tool failure. As the machining parameters were Average, it was not expected that this would occur, especially when machining commercial grade.

The carbides used to machine 3D Printed Ti-64 experienced wear. Tungsten was found present in the coated DNMG carbide; it can be seen in Figure 16 and Figure 17that the coating has failed. A very large BUE formed on the uncoated TNNG carbides.

As the Sandvik DNMG is a titanium coated carbide, it cannot be confirmed if diffusion of titanium occurred. Although if vanadium or aluminium is present on any cutting tool, some diffusion or a BUE has occurred. All specimens were found to have traces of Ti-64 and an area of carbon formation.

4.3.   Comparison of Ti-64 Swarf

4.3.1. Results

Figure 25 displays the swarf from 1st machining pass of machining commercial Ti-64 using a DNMG coated carbide using optimal machining parameters. Note the organic material – the small pieces scattered. The serration on the edge of the swarf is very mild – possibly caused by a coarse workpiece surface.

Figure 25 – 1st Optimal machining pass with DNMG carbide on commercial titanium.

Figure 26 displays similarly to above, however it is the 8th machining pass. The swarf has a very consistent width and ridge spacing. Only very slight spotting of serration occurring in the middle right of the image.

Figure 26 - 8th Optimal machining pass with DNMG carbide on commercial titanium.

42

Figure 27 displays the swarf from 1st machining pass of machining commercial Ti-64 using a DNMG coated carbide using Average machining parameters. Note the organic material illuminated white. The serration on the edge of the swarf is very severe. A combination of tool failure, and a poor workpiece surface. As this is the first pass of average machining, it cleaned up the 'rough' machining from optimal machining.
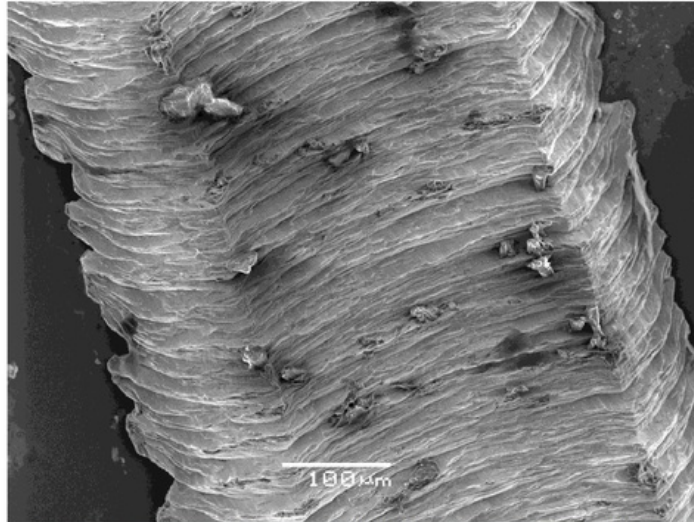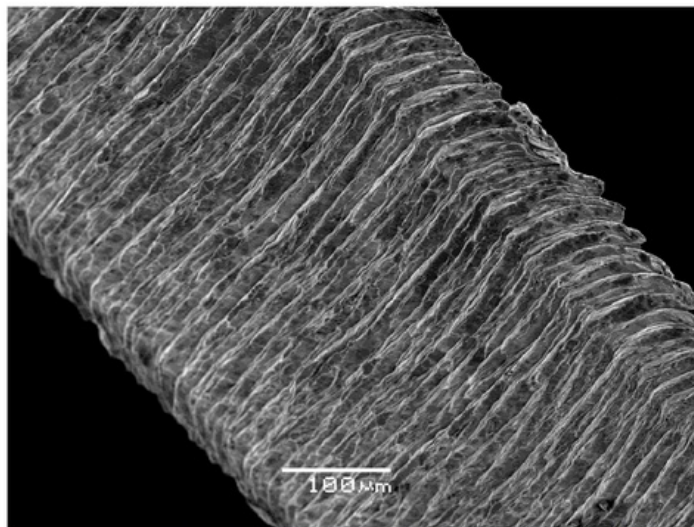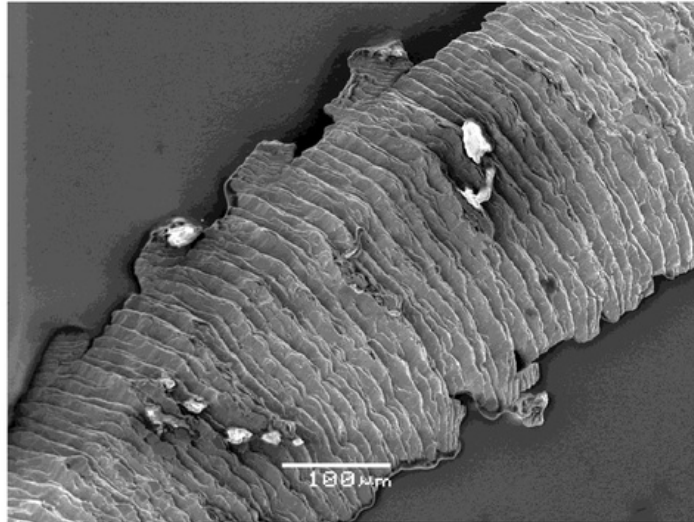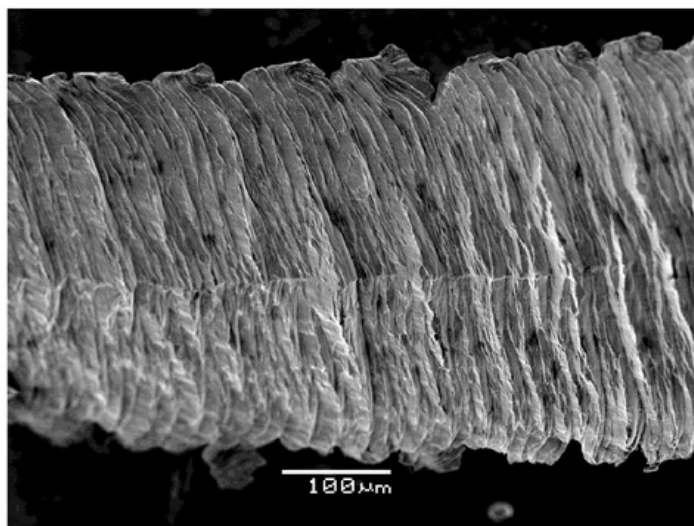

Figure 27 – 1st Average machining pass with DNMG carbide on commercial titanium.

Figure 28 displays similarly to above, however it is the 8th machining. The serration improves as there is a better surface to begin with, however tool failure is likely cause for the continued tearing.

Figure 28 - 8th Average machining pass with DNMG carbide on commercial titanium.

Figure 29 displays the swarf from 1st machining pass of machining commercial Ti-64 using a TNNG coated carbide using Optimal machining parameters. The width of this specimen of swarf is unusually thin, and has irregular ridge spacing. Some tearing of the bottom (convex) edge has occurred. The curvature of the specimen suggests the swarf curled tightly when machined.

Figure 29 – 1st Optimal machining pass with TNNG carbide on commercial titanium.

Figure 30 displays similarly to above, however it is the 8th machining. The width of the swarf is amongst the largest, as expected by using optimal parameters (slower feed). The geometry of the swarf is very consistent in width and ridge spacing. Note the white illuminated organic material.

Figure 30 –8th Optimal machining pass with TNNG carbide on commercial titanium.

44

Figure 31 displays the swarf from 1st machining pass of machining commercial Ti-64 using a TNNG coated carbide using Average machining parameters. Only the top edge of the swarf shows a very mild serration. Ridge spacing varies significantly.
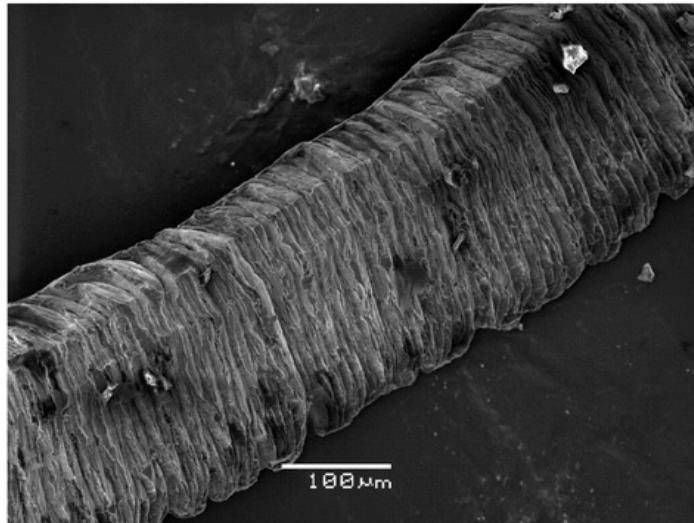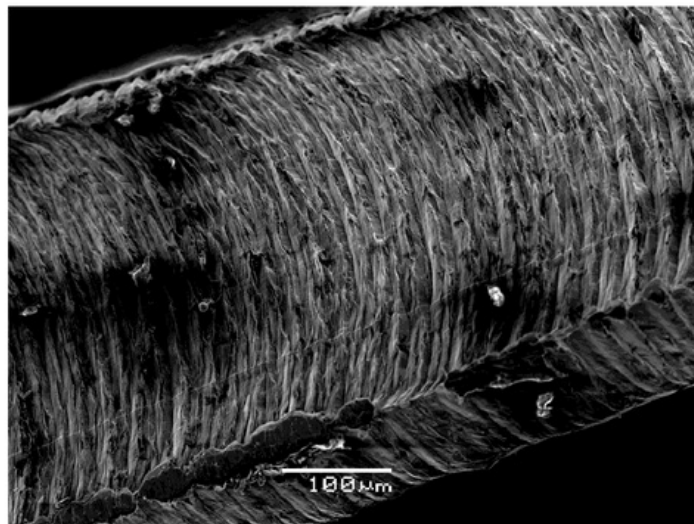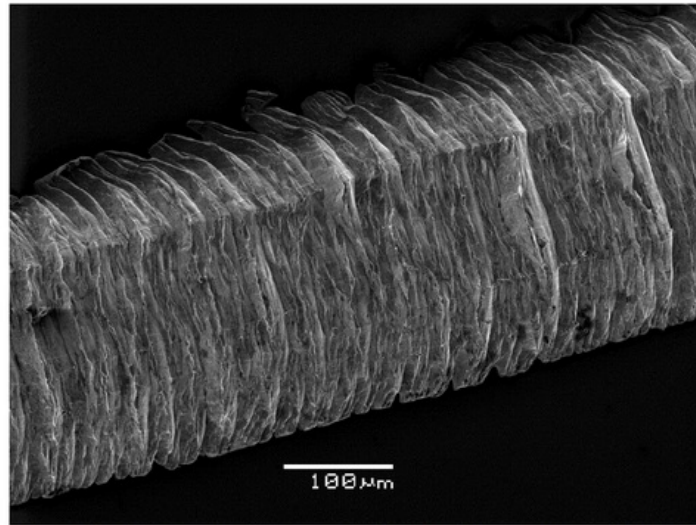

Figure 31 – 1ˢᵗ Average machining pass with TNNG carbide on commercial titanium.

Figure 32 displays similarly to above, however it is the 8th machining. The swarf is thin and curved suggesting it curled up when being machined. The outer edge displays heavy serration and very irregular ridge spacing.

Figure 32 – 8ᵗʰ Average machining pass with TNNG carbide on commercial titanium.

Figure 33 displays the swarf from 1st machining pass of machining SLM 3D Printed Ti-64 using a DNMG coated carbide using optimal machining parameters. Very heavy serration and tear out can be seen on the left of the swarf. The ridge spacing varies significantly when measuring from left to right. Additionally, large jumps in spacing occur when tear out is present.

Figure 33 – 1st Optimal machining pass with DNMG carbide on 3D printed titanium.

Figure 34 displays similarly to above, however it is the 8th machining pass. The width is much larger than the 1st pass and has some infrequent, yet significant serration. Ridge spacing varies in both the width and length of the swarf.

Figure 34 – 8th Optimal machining pass with DNMG carbide on 3D printed titanium.
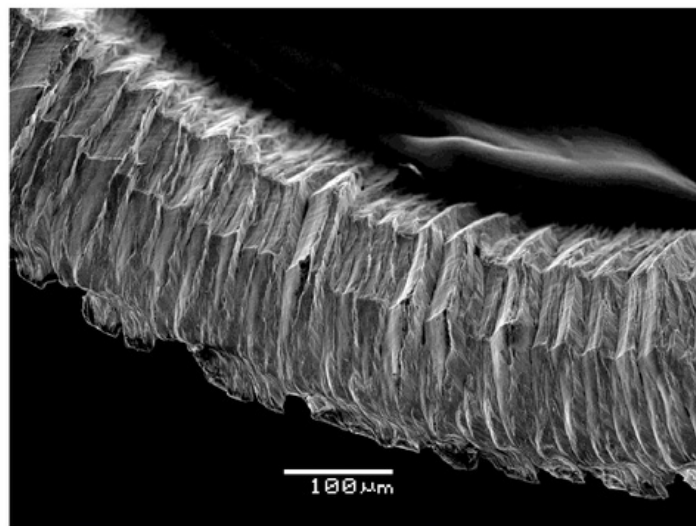
Figure 35 displays the swarf from 1st machining pass of machining SLM 3D Printed Ti-64 using a DNMG coated carbide using Average machining parameters. This specimen suffers the worst case of serration. The swarf is very thin in width, and ridge spacing is very consistent.
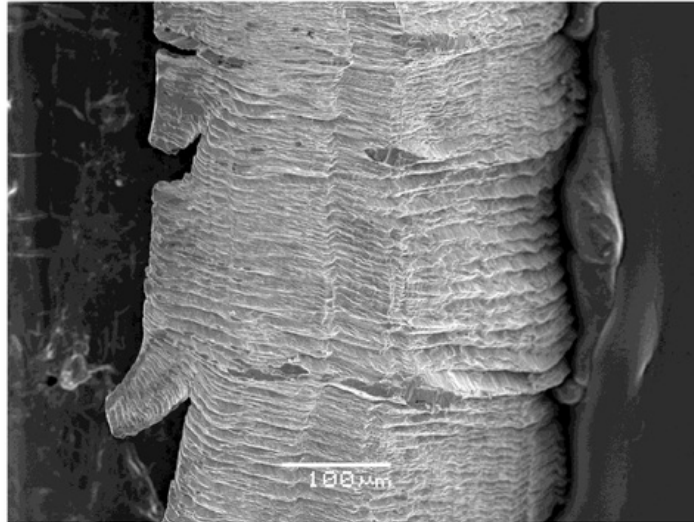

Figure 35 – 1ˢᵗ Average machining pass with DNMG carbide on 3D printed titanium.

Figure 36 displays similarly to above, however it is the 8th machining pass. This specimen of swarf has grown slightly in width compared to Figure 35. Ridge spacing is consistent and very slight serration on the right hand side.
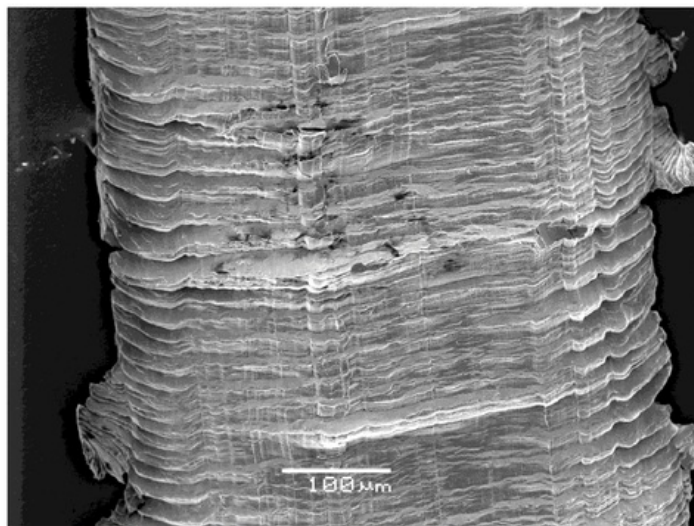

Figure 36 – 8ᵗʰ Average machining pass with DNMG carbide on 3D printed titanium.

Figure 37 displays the swarf from 1st machining pass of machining SLM 3D Printed Ti-64 using a TNNG coated carbide using Optimal machining parameters. The ridge spacing is very inconsistent, and quite large. No serration has occurred.
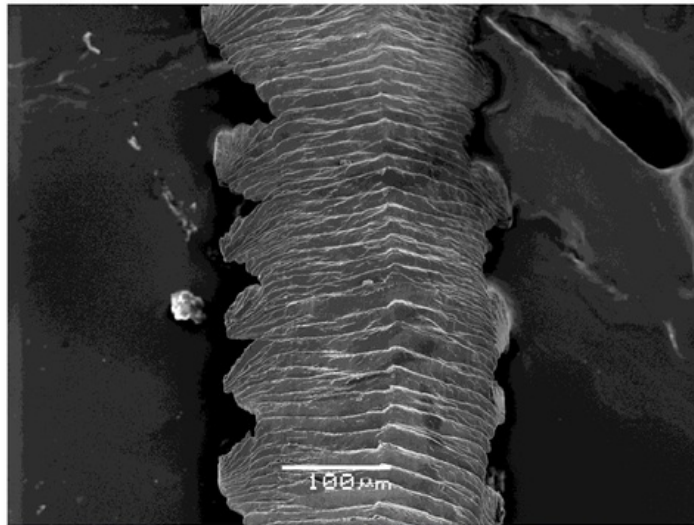

Figure 37 – 1st Optimal machining pass with TNNG carbide on 3D printed titanium.

Figure 38 displays similarly to above, however it is the 8th machining pass. No serration is evident, which may be due to the viewing perspective as the swarf looks concave. The ridge spacing is quite large, and the width is greater than the 1st machining pass.
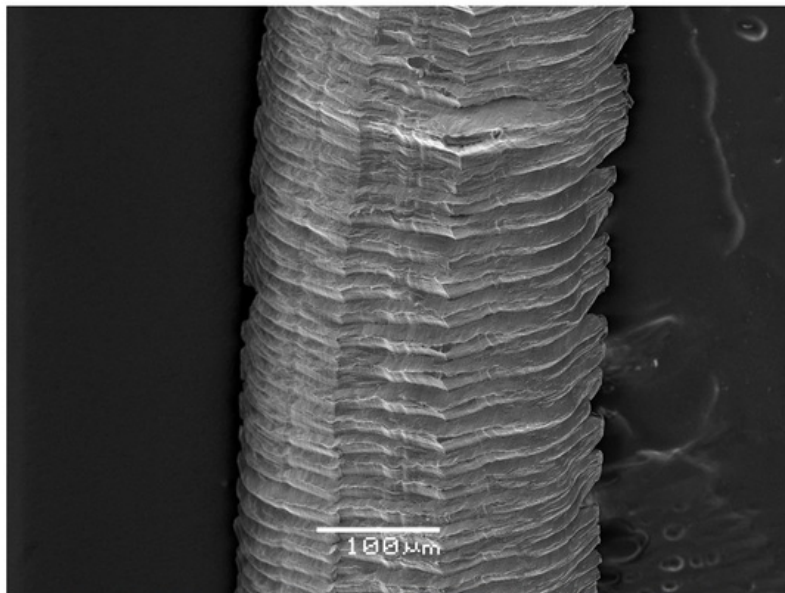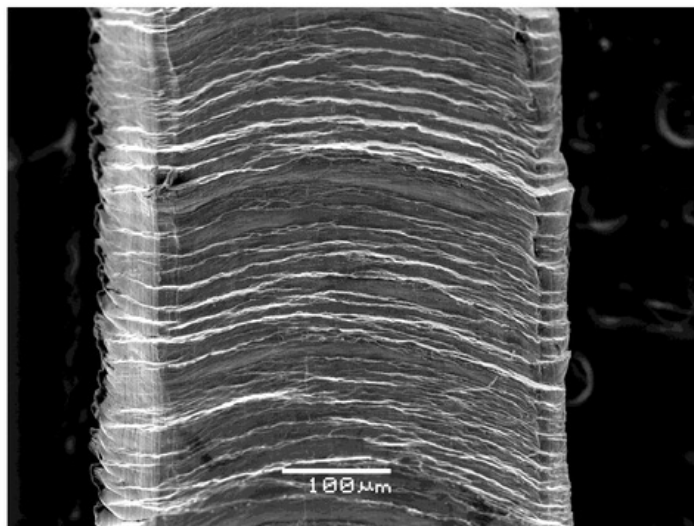

Figure 38 – 8th Optimal machining pass with TNNG carbide on 3D printed titanium.

Figure 39 displays the swarf from 1st machining pass of machining SLM 3D Printed Ti-64 using a TNNG coated carbide using Average machining parameters. Large serration can be seen on the right hand side of the swarf, lessening in size on the left. The ridge spacing is very tight towards the bottom and gradually gets larger towards the top.
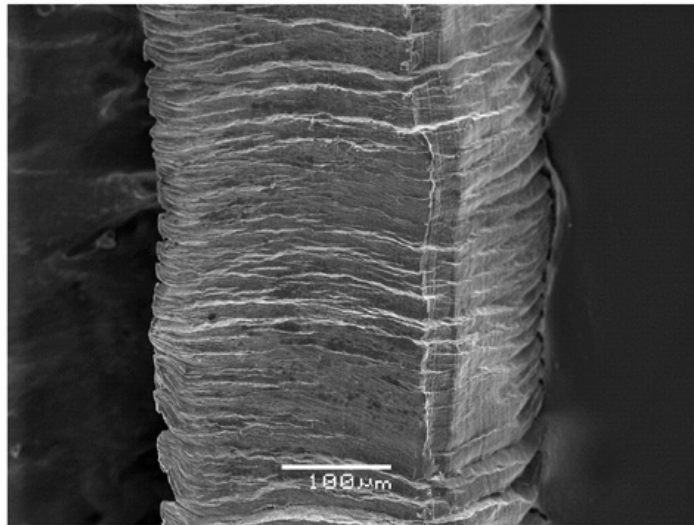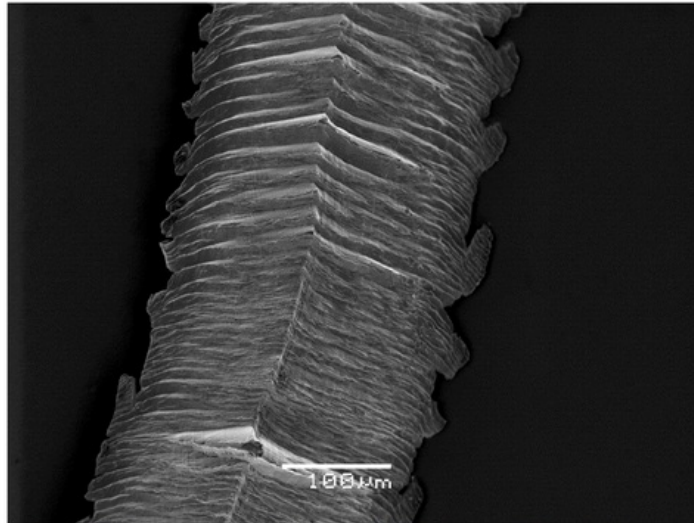

Figure 39 – 1st Average machining pass with TNNG carbide on 3D printed titanium.

Figure 40 displays similarly to above, however it is the 8th machining pass. The width is much larger than the 1st machining pass, and has one of the largest ridge spacing. Lots of carbon can be seen in this image, denoted by the black areas (on the swarf).
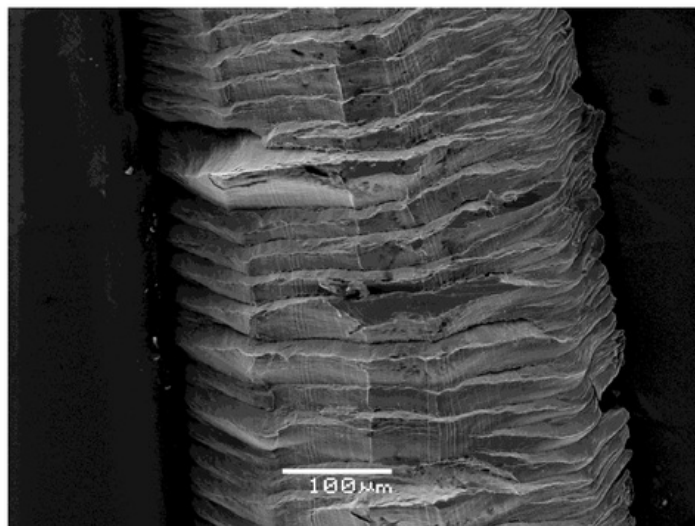
Figure 40 – 8th Average machining pass with TNNG carbide on 3D printed titanium.

Figure 41 shows the difference in swarf width based on the data found in Table 8. It displays the sizing of the 1st and 8th machining pass on the left and right respectively when machining SLM 3D printed Ti-64. The lines show that as the machining continued, the swarf grew in size.

Figure 41 - Displays the difference in swarf width between 1st and 8th machining pass of 3D printed Ti-64

Table 8 displays the dimensions of the swarf width and ridge spacing for the 1st and 8th machining pass of both commercial and 3D printed Ti-64.

Table 8 - Comparison of swarf width and ridge spacing.

Machining Operation	Machining Pass	Commercial Ti-64		3D printed Ti-64	
		Swarf Width (µm)	Ridge Spacing (µm)	Swarf Width (µm)	Ridge Spacing (µm)
DNMG Optimal	1	494	21	377	6
	8	429	19	511	15
DNMG Average	1	286	17	229	14
	8	353	16	292	13
TNMG Optimal	1	241	13	358	22
	8	441	16	433	18
TNMG Average	1	289	21	285	15
	8	228	34	400	26

4.3.2. Discussion

4.3.2.1.   Sample Preparation

The swarf was collected after the first and the eighth machining pass of each material, carbide and machining parameter. The swarf was bagged and catalogued.

Before analysis, the swarf was broken down into a smaller size and then cleaned with acetone. The swarf was mounted on small aluminium stubs. Any step following solvent cleaning required use of surgical gloves.

4.3.2.2.   Swarf Sizing

The quantitative data gained from measuring the swarf width and ridges spacing was completed with the program BigPrint. It is a scaling program designed for printing 1:1 scaled images. It also functions as a measurement tool given a reference dimension. As the swarf varies so much in size, an average of 3 measurements was taken, all a varying distance away from one another. Table 8 describes the average width of the swarf and the average ridge spacing. The width of the swarf is determined by the depth of cut and feed rate. As the depth of cut is controlled, the feed rate determines the width of the swarf. The area of the cutting edge increases when using a quicker feed rate, additionally the cutting force increases resulting in shorter tool life. Results shows that a faster feed rate removes more material; that is, Optimal machining produces swarf with a larger width.

Another trend was the increase in swarf width after 8 machining passes, with two exceptions – commercial DNMG Optimal, and commercial TNNG Average.

During machining, the 3D printed Ti-64 experienced noticeable deflection. The combination of the material being hard and thin, and the generation of heat allowed the tip of the workpiece to flex, removing less material than towards the end of the cut.

Figure 40 demonstrates that on average, the swarf from machining 3D printed Ti-64 grew at twice the rate that occurred from commercial grade, measuring between the first and eighth machining pass. Similarly, machining with optimal parameters grew twice the rate than when using average.

Ridges are caused by the compaction of material when being cut by the carbide. The closer packed the ridges, the more force required to remove material. Greater force when machining results in a shorter tool life, and worse surface finish.

The trend found by plotting the difference in ridge spacing showed that a DNMG carbide decreased the size of the ridge spacing, conversely, the spacing increased when using a TNNG carbide. Additionally TNNG produced swarf with the largest ridge spacing. Results show the ridge spacing is not depended on the machining parameters used.

No conclusion can be drawn regarding the swarf ridge spacing as no trend was found whether comparing the material, carbide or machining parameter used.

4.3.2.3. Swarf Serration

Select swarf samples experienced tearing on the edge creating a serration on the edge. Qualitative analysis suggests that as machining continues the serration improves. I.e. the serration from the 1st machining pass is less significant after the 8th machining pass. The only exception is when machining commercial grade Ti-64 using a TNNG carbide using average machining parameters.

Generally the cause for serration of swarf is due to poor cutting. However, as serration subsides, the only parameter changes is the increased heat from machining. The heat increase could cause expansion/elastic behaviour somehow improving the cutting.

The worst cases of serration occurred on the 1st pass using a DNMG carbide. The material does not influence the severity or occurrence of serration.

4.3.2.4. Diffusion

EDS analysis was done on all chips in attempt to identify if any diffusion from the cutting tools had occurred. There was no diffusion of the TNNG carbide, as no tungsten was detected in any of the swarf samples. There is no conclusive answer whether diffusion of the DNMG tungsten occurred as the coating is titanium carbo-nitride and if diffusion did occur, it would be present as titanium or nitrogen, which is already present in the base metal. While negligible trace amounts (<0.1wt %) of nitrogen were found in very few samples, it is too small of a value to be considered.

EDS analysis can be seen on both a commercial and 3d Printed Ti-64 swarf in appendix; see section 8.3.2.

5. Summary

Material Composition

SLM 3D printed Ti-64 displayed very consistent values of composition, due to the material used and manufacturing process of said material. Three points of analysis was completed on the specimen, all values were within 2wt%. The hardness of the material was measured at 392 HV5.

Analysis on commercial grade Ti-64 varied significantly due to the microstructure of the material. An overview measurement confirmed the specimen was consistent with an inspection certificate that arrived with the titanium bar. Specific points were identified as alpha and beta phase, consisting of varying quantities of aluminium and vanadium. The hardness of the material was measured at 312 HV5.

Cutting Tool - Tool failure and BUE

The TiCN coated Sandvik DNMG carbide performed well for a tool not designed to machine titanium. The coating was intact after 8 passes of machining commercial Ti-64. However, failure of the coating did occur when optimally machining 3D Printed Ti-64.

The uncoated Kyocera TNNG carbide did have large formations of carbon present when machining commercial Ti-64. The tool did experience failure when machining commercial Ti-64 using average machining parameters.

A large BUE formed on the edge on the Kyocera TNNG cutting tool when machining 3D printed Ti-64. Titanium alloy was present on all carbides analysed.

Swarf – Diffusion and sizing

No diffusion occurred between the uncoated carbide (Kyocera TNNG) and the swarf as no tungsten was detected in the swarf samples.

It is inconclusive if diffusion of the coated carbide (Sandvik DNMG) occurred as the coating is a titanium carbo-nitride; Titanium and trace nitrogen is present in the base material, so if any diffusion did occur, it could not be detected.

The width of swarf produced when machining 3d printed Ti-64 grew 30% when comparing between the 1st and 8th machining pass.

6. Future Work

The results gathered provide a foundation for machining 3D printed Ti-64. If further research on the machinability of Ti-64 is performed, a suggested direction includes:

- Heat treatment of commercial grade Ti-64 to introduce some martensite into the microstructure and compare the machinability to the 3D Printed Ti-64. This would identify if the characteristics of machining 3D printed Ti-64 is specific to the microstructure or the manufacturing process.

- Use a carbide that does not contain any titanium in the coating. Then diffusion could be tested on a coated carbide.

- Obtain an SEM or roughness measurement tool to check the roughness of the carbide. Then the wear rate/roughness could be measured.

- Use a different machining parameter and depth of cut. The suggested machining parameters used from Machinery's Handbook does not include the parameters for a smooth enough 'finishing' pass.

7. References

[1] Kathy, "The Most Fascinating Titanium Uses," 7 September 2011. [Online]. Available: http://titanium.com/2011/09/07/the-most-fascinating-titanium-uses/. [Accessed 1 September 2016].

[2] E. O. EZUGWU and Z. M. WANG, "Titanium alloys and their machinability - a review," *Materials Processing Technology,* vol. 68, pp. 262-274, 1997.

[3] S. Seong, O. Younossi and B. W. Goldsmith, "Titanium Industrial Base, Price Trends, and Technology Initiatives," 2009. [Online]. Available: http://www.rand.org/content/dam/rand/pubs/monographs/2009/RAND_MG789.pdf. [Accessed 1 September 2016].

[4] B. Godbey, "Surface Finish Control of 3D Printed Metal Tooling," Clemson University, 2007.

[5] M. RAHMAN, Y. S. WONG and R. ZAREENA, "Machinability of Titanium Alloys," *JSME International Journal,* vol. 46, no. 1, pp. 107-115, 2003.

[6] E. Oberg, F. D. Jones, H. L. Horton and H. H. Ryffel, Machinery's Handbook, 27th, Ed., New York: Industrial Press Inc., 2004.

[7] AZO Materials, "AZO Materials," [Online]. Available: http://www.azom.com/article.aspx?ArticleID=1547. [Accessed 5 May 2016].

[8] I. SHANE, I. MARKUS and W. JEONG, "New Cooling Approach and Tool Life Improvement in Cryogenic Machining of Titanium Alloy Ti-6Al-4V," *International Journal of Machine Tools&manufacture,* vol. 41, pp. 2245-2260, 2001.

[9] RMI Titanium Company, "Titanium Alloy Guide," [Online]. Available: www.RMITitanium.com. [Accessed 5 May 2016].

[10] 3D Printing, "Understanding 3D Printing Titanium," [Online]. Available: http://3d-printing-titanium.com/. [Accessed 1 Oct 2016].

[11] T. Baumelster, E. Avallone and T. Baumelster III, Mark's Standard Handbook for Mechanical Engineers, McGraw Hill, 8th.

[12] ME Mechanical Team, "Built up Edge," 19 April 2016. [Online]. Available: http://me-mechanicalengineering.com/built-up-edge/. [Accessed 1 September 2016].

[13] M. Free, "Built Up Edge - What it is and What to do," [Online]. Available: https://pmpaspeakingofprecision.com/2010/10/07/built-up-edge-what-it-is-and-what-to-do/. [Accessed 1 September 2016].

[14] T. Alam, "BUE formation during machining," 26 August 2016. [Online]. Available: http://mechanical-engg.com/blogs/entry/950-bue-formation-during-machining/. [Accessed 1 September 2016].

[15] WorkSafe Victoria, "Safe use of metal turning lathe," September 2010. [Online]. Available: https://www.worksafe.vic.gov.au/__data/assets/pdf_file/0016/12148/GN2BTurning2BLathes_web.pdf. [Accessed 1 September 2016].

[16] D. A. Stephenson and J. S. Agapiou, Metal Cutting Theory and Practice, New York: Marcel Dekker Inc, 1996.

[17] M. BELTRAME, E. KULJANIC, M. FIORETTI and F. MIANI, "Titanium Alloy Turbine Blades Milling with PCD cutter," *Advanced Manufacturing Systems and Technology,* pp. 121-128, 1996.

[18] ASM International, "Metals Handbook," vol. 9, p. 16, 1989.

[19] J. F. Kahles, M. Field, D. Eylon, F. H. Froes and J. Met, "Machining of Titanium Alloys," vol. 37, no. 4, pp. 27-35, 1985.

[20] Sandvik, "Formulas and Definitions," Sandvik, [Online]. Available: http://www.sandvik.coromant.com/en-gb/knowledge/general_turning/formulas-and-definitions?Country=au. [Accessed 1 September 2016].

[21] Stuers, "e-Metalog Titanium Alloys (DiaPro)," Struers, [Online]. Available: https://e-shop.struers.com/DK/EN/methods/Non-Ferrous_Metals/Titanium_and_Ti_Alloys/Titanium_Alloys_(DiaPro_Application_Note)(1417).aspx. [Accessed 1 Sep 2016].

[22] D. McMullan, "Scanning Electron Microscopy 1928-1965," August 1993. [Online]. Available: http://www-g.eng.cam.ac.uk/125/achievements/mcmullan/mcm.htm. [Accessed 1 September 2016].

[23] Australian Microscopy & Microanalysis Research Facility, "Background Information - What is energy dispersive xray spectroscopy?," AMMRF, 12 June 2014. [Online]. Available: http://www.ammrf.org.au/myscope/analysis/eds/. [Accessed 1 September 2016].

[24] Sandvik, "DNMG 11 04 04-PM 4225," Sandvik, [Online]. Available: http://www.sandvik.coromant.com/en-us/products/Pages/productdetails.aspx?c=dnmg+331-pm+4225#?query=%7B%22n%22:%22Insert%22,%22l%22:%22%22,%22r%22:%5B%5D,%22c%22:%5B%5D%7D. [Accessed 2016 Oct 1].

[25] Kyocera, "Kyocera grade SW05," [Online]. Available: http://www.kyoceramicrotools.com/indexable/pdf/PR13-Series_and_SW05_for_Heat_Resistant_Alloys_W.pdf. [Accessed 2016 Oct 1].

[26] W. R. R. R KOMANDURI, "Evaluation of Carbide Grades and a New Cutting Geometry for Machining Titanium Alloys," vol. 92, pp. 113-123, 1983.

[27] J. WAITER, D. W. SKELLY and W. P. MINNEAR, "Wear," pp. 79-82, 1993.

[28] Z.-C. LIN and K.-Y. CHEN, "A Study with a CBN Tool," *Journal of Materials Processing Technology,* vol. 49, pp. 149-164, 1995.

[29] T. MAEKAWA, A. KITAGAWA and K. KUBO, "Temperature and Wear of Cutting Tools in High Speed Machining of Inconel and Ti-6Al-6V," pp. 142-148, 1997.

[30] H. SCHULZ and T. MORIWAKI, "High Speed Machining," *Annals CIRP,* vol. 41, pp. 637-643, 1992.

[31] South Bay Machine, "South Bay Machine," 1990. [Online]. Available: http://www.southbaymachine.com/setups/cuttingspeeds.htm#Feed Rates. [Accessed 5 May 2016].

[32] A. R. MACHADO, J. WALLBANK and I. R. PASHBY, "Tool Performance and Chip Control when Machining Ti-6Al-4V and Inconel Using High Pressure Coolant," *Machining Science and Technology,* vol. 2, no. 1, pp. 1-12, 1998.

[33] A. R. MACHADO and J. WALLBANK, "Machining of Titanium and its alloys - a review," *Proc Instn Mech Engineers,* vol. 204, pp. 53-60, 1990.

[34] B. L. DUTROW and C. M. CLARK, "Geochemical Instrumentation and Analysis," Eastern Michigan & Louisiana State University, [Online]. Available: http://serc.carleton.edu/research_education/geochemsheets/techniques/XRD.html. [Accessed 5 May 2016].

[35] H. Z. Loye, "X-ray Diffraction," University of South Carolina, [Online]. Available: http://www.chem.sc.edu/faculty/zurloye/xrdtutorial_2013.pdf. [Accessed 5 May 2016].

[36] S. Mukhopadhyay, "Sample Preparation for microscopic and spectoscopic characterisation of solid surfacs," [Online]. Available: http://www.spectroscopynow.com/userfiles/sepspec/file/specNOW/Tutorials/sample_prep_mitra_377-412.pdf. [Accessed 5 May 2016].

[37] N. ZLATIN, "Modern Machine Shop," vol. 42, no. 12, pp. 139-144, 1970.

[38] B. L. Dutrow, "Geochemical Instrumentation and alysis," [Online]. Available: http://serc.carleton.edu/research_education/geochemsheets/techniques/XRD.html.

[39] R. Steinard, "Iscar Chip Formation," 11 February 2012. [Online]. Available: https://www.youtube.com/watch?v=mRuSYQ5Npek. [Accessed 1 September 2016].

[40] Cartech, "Titanium Alloy Ti 6Al-4V Technical Datasheet," Dynamet Holdings Inc, 1 July 2000. [Online]. Available: https://cartech.ides.com/datasheet.aspx?i=101&E=269. [Accessed 1 September 2016].

[41] Peaking Precision, "Built upo edge what is it and what to do," [Online]. Available: https://pmpaspeakingofprecision.com/2010/10/07/built-up-edge-what-it-is-and-what-to-do/.

8. Appendix

8.1. Ti-64 Compositional Analysis

Table 9- Hardness test results of 3D Printed Ti-64

3D TI-64

TEST	A	B	C	Mean	Overall Mean	Standard Deviation	Standard Error
1	404	385	403	397		11	6
2	391	384	376	384		8	4
3	387	401	395	394	392	7	4
4	398	399	398	398		1	0
5	381	381	381	381		0	0
6	399	397	399	398		1	1

Table 10 - Hardness test results of commercial grade Ti-64

COMMERCIAL TI-64

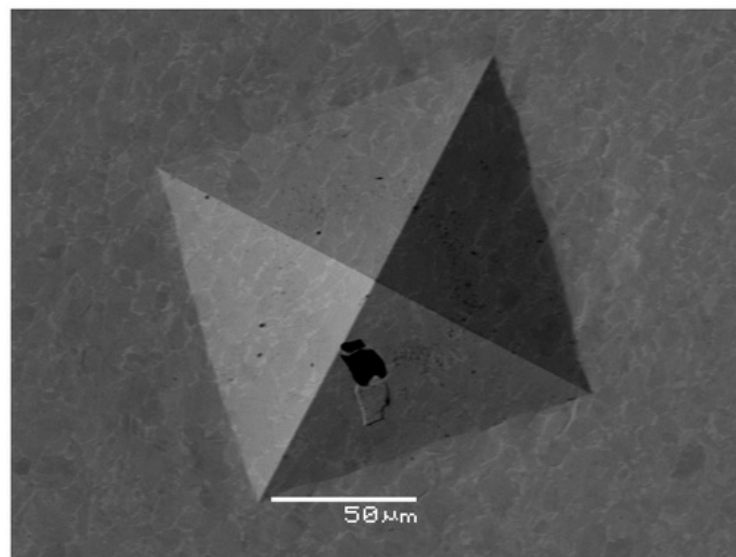| TEST	A	B	C	Mean	Overall Mean	Standard Deviation	Standard Error
1	318	311	313	314		3.605551	2.081666
2	306	312	311	310		3.21455	1.855921
3	310	310	313	311	312	1.732051	1
4	313	314	314	314		0.57735	0.333333
5	315	308	313	312		3.605551	2.081666
6	317	311	315	314		3.05505	1.763834

Figure 42 - Hardness Test crater imaging of commercial Ti-64.
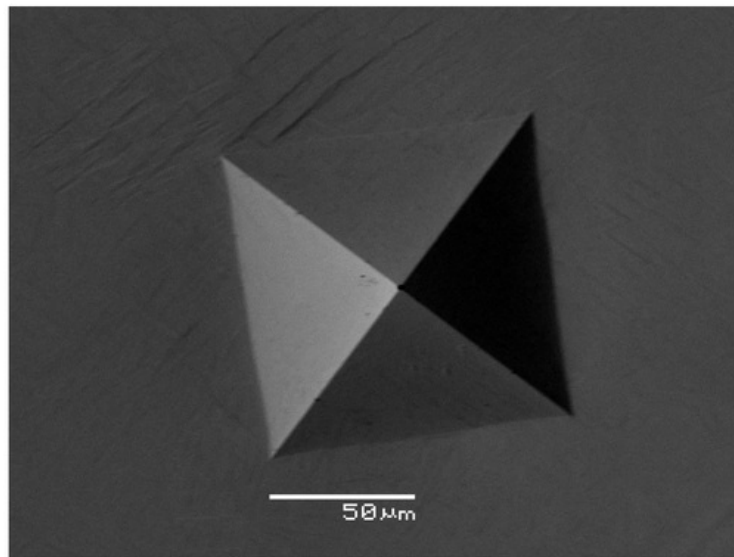
Figure 43 - Hardness test crater imaging of SLM 3D printed Ti-64

INSPECTION CERTIFICATE

Date: 16/9/2014	Customer:		Order No:		Our Ref: 0C215153		CERTIFICATE NUMBER: HX-MTC-14015
GRADE:	SIZE:		SPECIFICATION:		HEAT NUMBER:		BATCH NUMBER:
TITANIUM GR-5	38.1MM DIA		ASTM B-348-2013 GRADE -5 Ti-6Al-4V		H14081401		H201406-042

CHEMICAL ANALYSIS

ELEMENTS %	N	C	H	Fe	O	Al	V	Ti	OTHER				
Final Product analysis	0.015	0.016	0.001	0.17	0.14	6.20	4.26	BAL	0.4				

MECHANICAL TEST

Tensile Strength MPa	Yield Strength MPa	ELONGTION %	Reduction of Area	Temper	Remarks:PASS Visual Inspection:PASS Dimensional Inspection:PASS
985	900	16	44		

We hereby affirm that the reported results are true and correct copies of the original mill certificate held in our possession in accordance with EN 10204 3.1
All tests, results and operations performed by Specialty Metals or its subcontractors are in compliance with the applicable material/customer specifications.

QUALITY MANAGER:

Unit 1, 14 Moriarty Road, Welshpool WA 6106
t : +61 8 9353 5588   f : +61 8 9353 5599   www.specialtymetals.com.au

Figure 44 - Inspection certificate of the purchased Ti-64 bar displaying the composition.
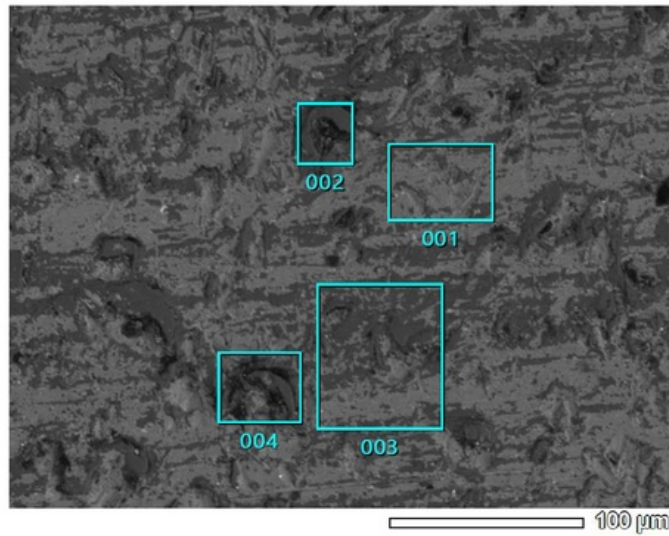
8.2.   Test holder

Figure 45 - EDS area analysis map of aluminium screw vice. Magnification is 370x.
The image was taken using a backscatter detector to identify different elements
present.

Table 11 - EDS Analysis of Figure 45, the aluminium screw test holder displaying the Weight% of each element for the
respective areas. Note the appearance of gold – due to gold sputter coating for non-conductive material.

Test Holder

Element	1	2	3	4
Carbon	15.69	28.41	17.26	32.24
Nitrogen		3.69		3.37
Oxygen	3.82	6.68	4.83	8.42
Aluminium	70.94	60.47	71.99	52.41
Silver	1.5			
Gold	8.06		5.92	3.56

8.3.   EDS Analysis
8.3.1. Carbide Cutting Tools

Table 12 – EDS analysis for reference Sandvik DNMG and Kyocera TNNG.

DNMG

	1	2	3	4
Carbon	7.68	22.68	12.03	51
Nitrogen	12.27	7.38	6.53	10.55
Oxygen	5.28	11.03	3.57	12
Aluminium	0.86	28.19	0.65	0.34
Titanium	72.95	21.01	75.75	19.98
Vanadium	0.54	9.7	0.69	0.27
Tungsten			0.14	

TNNG

	1	2	3	4	5
Carbon	68.14	60.54	5.7	10.4	8.26
Silicon	21.44				
Iron			57.04		
Tungsten		9.36		89.6	91.74
Nickel			17.01		
Chromium			17.35		

Table 13 - EDS analysis data for a DNMG carbide machining commercial grade Ti-64

Commercial **DNMG**							
Optimal	1	2	3	4	5	6	7
Carbon	9.41	36.41	24.58	76.73	47.74	8.04	7.31
Nitrogen	26.2			22.26	12.88		
Oxygen	7.9	9.56				6.96	
Aluminium	1.05	51.56	5.58	0.24	2.86	4.96	6
Titanium	54.21		67.6	0.72	32.65	76.39	82.92
Vanadium	0.46	2.47	2.1		1.53	3.49	3.71
Tungsten	0.3		0.14	0.04	0.34	0.16	0.06
Average	8	9	10	11	12	13	
Carbon	9.84	10.58	40.09	71.94	41.59	15.15	
Nitrogen		22.16	9.61	14.76	17.3	6.56	
Oxygen	3.9	8.68	13.44	4.52	17.3	9.91	
Aluminium	4.65	7.12	8.56	4.38	2.16	8.54	
Titanium	77.18	49.67	23.42	4.39		53.91	
Vanadium	3.49	0.24	0.29			2.31	
Tungsten		0.16				0.11	

Table 14 - EDS analysis data for a TNNG carbide machining commercial Ti-64

Commercial	TNNG					
Optimal	2	3	4	5	6	
Carbon	23.33	74.94			43.5	
Nitrogen		24.81				
Oxygen					17.81	
Aluminium	2.78	0.02			3.09	
Titanium	41.08				33.31	
Vanadium						
Tungsten	31.45	0.23			2.29	
Average	1	2	3	4	5	6
Carbon	6.84	74.67	9.93	8.68	1.64	12.5
Nitrogen		19.78				
Oxygen		5.55	11.06	5.38	1.37	6.11
Aluminium	5.74		5.23		4.26	0.66
Titanium	82.89		73.33	1.14	86.78	8.44
Vanadium	4.36				4.34	0.12
Tungsten	0.18		0.1	84.19	0.12	70.18

Table 15 - EDS analysis data for a DNMG carbide machining 3D printed Ti-64

3D Printed	DNMG				
Optimal	1	2	3	4	
Carbon	49.99	19.17	14.61	6.32	
Nitrogen	9.94	7.38			
Oxygen	13.82	6.07	4.61	1.93	
Aluminium	1.49	1.29	4.75	5.17	
Titanium	13.17	21.89	72.91	83.05	
Vanadium	0.56	1.01	3.12	3.4	
Tungsten	0.06	39.06		0.13	
Average	1	2	3	4	5
Carbon	19.33	6.89	44.87	5.52	54.86
Nitrogen	6.71		12.22		16.6
Oxygen	29.34	2.02	28	2.58	13.89
Aluminium	35.54	5.24	1.6	5.27	2.12
Titanium	7.56	82.51	0.64	83.41	6.98
Vanadium	0.3	3.28	0.06	3.17	0.41
Tungsten	0.24	0.05	0.24	0.05	

Table 16 - EDS analysis data for a TNNG carbide machining 3D printed Ti-64

3D Printed	TNNG					
Optimal	1	2	3	4	5	6
Carbon	6.95	6.16	55.97	11.76	17.8	3.97
Nitrogen	2.27		14.06			
Oxygen	1.52	2.2	16.66	4.83	8.91	2.62
Aluminium	0.39	5.8	0.24	5.62	4.76	5.2
Titanium	6.21	82.22	0.6	73.88	63.74	74.91
Vanadium	0.28	3.39		3.3	2.97	3.06
Tungsten	82.29	0.23	0.3	0.15	0.14	10.23
Average	1	2	3	4		
Carbon	53.57	6.53	12.42	5.83		
Nitrogen	14.83		2.85			
Oxygen	18.57	2.14	2.8	4.25		
Aluminium	5.27	5.58	0.59	5.64		
Titanium	0.78	77.79	6.61	80.23		
Vanadium	0.19	5.33	0.35	2.91		
Tungsten	0.11	0.12	73.45	1.15		

8.3.2. Swarf

Since the swarf EDS analysis is similar to the composition of the base metal, only two specimens are shown.
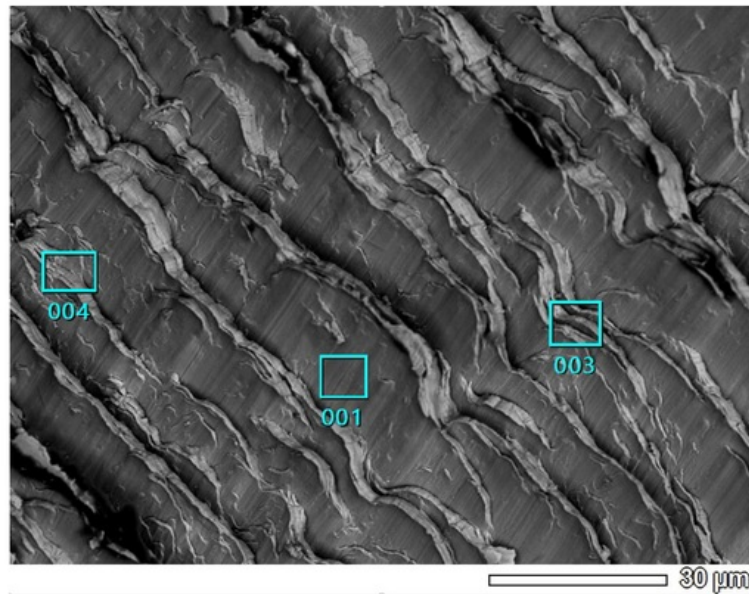
Figure 46 - Swarf from machining commercial Ti-64 using a DNMT carbide and using Average machining parameters

Figure 47 - Swarf from machining commercial Ti-64 using a DNMT carbide and using Average machining parameters

Table 17 - EDS analysis for a commercial ti-64 swarf after being machined with a DNMT carbide using average machining parameters.

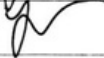| DNMT	Average	Commercial	1st
Element	1	2	3
Carbon	1.8	2.01	1.19
Nitrogen			
Oxygen	2.54	5.93	3.51
Aluminium	0.72	3.38	2.71
Titanium	94.94	83.94	89.55
Vanadium		4.54	3.04
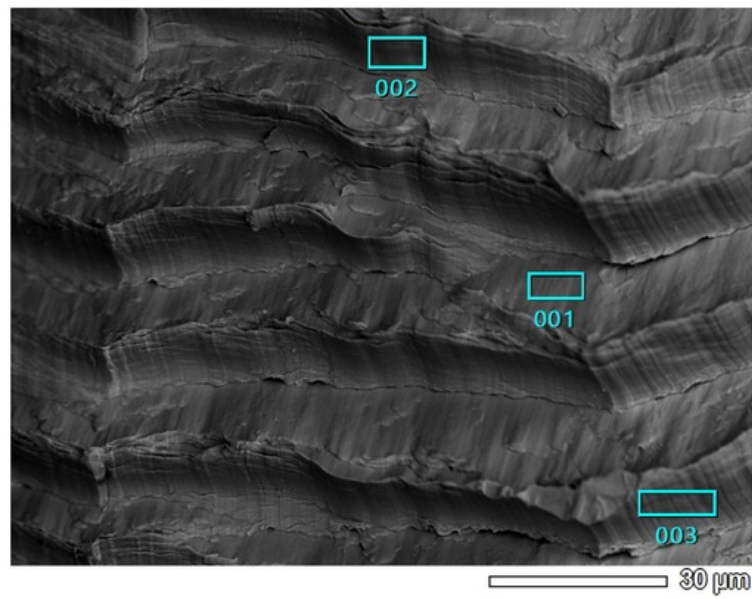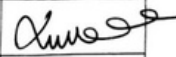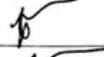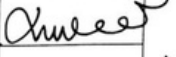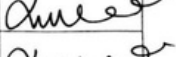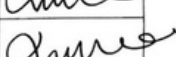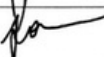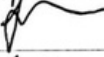
Figure 48- Swarf from machining 3D Printed Ti-64 using a DNMT carbide and using Average machining parameters

Figure 49- Swarf from machining 3D Printed Ti-64 using a DNMT carbide and using Average machining parameters

Table 18 - EDS analysis for a 3D printed ti-64 swarf after being machined with a DNMT carbide using average machining parameters.

DNMT	Average	3D Printed	8th
Element	1	2	3
Carbon	1.03	1.69	1.38
Nitrogen	0.07		
Oxygen	0.34	1.11	1.59
Aluminium	0.08	0.52	1.62
Titanium	94.56	92.12	90.47
Vanadium	3.92	4.57	4.93

Consultation Meetings Attendance Form

Week	Date	Comments (if applicable)	Student's Signature	Supervisor's Signature
-2	11/7/16	Met with wei - new project supervisor		
-1	18/7/16	Talked about material costing		
0	25/7/16	Material arrived Discussed Carbides to be used		
1	1/8/16	3D SLM Ti-64 sample to compare		
3	15/8/16	Planning for experiment		
4	23/8/16	Phenom SEM demonstration		
6	7/9/16	Discussed experimental plan		
7	16/9/16	Discussed pricing EDS/SEM		
9	10/10/16	Email progress job w/ Mets put in		
10	20/10/16	Email wei update on SEM results		
12	3/11/16	Email all results complete		
13	7/11/16	Advice on Thesis Report		